AD NUMBER
ADB002257
LIMITATION CHANGES

TO:

Approved for public release; distribution is unlimited.

FROM:

Distribution authorized to U.S. Gov't. agencies only; Test and Evaluation; FEB 1975. Other requests shall be referred to Armament Development Test Center, Attn: SDTT, Eglin AFB, FL 32542.

AUTHORITY

AFATL ltr 23 May 1977

AEDC-TR-75-17
AFATL-TR-75-27

CALIBRATIONS OF ANGLE-OF-ATTACK, ANGLE-OF-SIDESLIP, AND PITOT-STATIC PRESSURE SENSORS ON THE MODULAR-GUIDED GLIDE BOMB II AT TRANSONIC MACH NUMBERS

D. A. MacLanahan, Jr.
ARO, Inc.

PROPULSION WIND TUNNEL FACILITY
ARNOLD ENGINEERING DEVELOPMENT CENTER
AIR FORCE SYSTEMS COMMAND
ARNOLD AIR FORCE STATION, TENNESSEE 37389

February 1975

Final Report for Period September 23 — 26, 1974

Prepared for

ARMAMENT DEVELOPMENT TEST CENTER (SDTT)
EGLIN AIR FORCE BASE, FLORIDA 32542

APPROVAL STATEMENT

This technical report has been reviewed and is approved for publication.

FOR THE COMMANDER

LAMAR R. KISSLING
Lt Colonel, USAF
Chief Air Force Test Director, PWT
Directorate of Test

FRANK J. PASSARELLO
Colonel, USAF
Director of Test

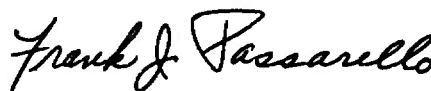| REPORT DOCUMENTATION PAGE		READ INSTRUCTIONS BEFORE COMPLETING FORM
1 REPORT NUMBER AEDC-TR-75-17 AFATL-TR-75-27	2. GOVT ACCESSION NO.	3 RECIPIENT'S CATALOG NUMBER
4 TITLE (and Subtitle) CALIBRATIONS OF ANGLE-OF-ATTACK, ANGLE-OF-SIDESLIP, AND PITOT-STATIC PRESSURE SENSORS ON THE MODULAR-GUIDED GLIDE BOMB II AT TRANSONIC MACH NUMBERS		5 TYPE OF REPORT & PERIOD COVERED Final Report - September 23 - 26, 1974
		6. PERFORMING ORG REPORT NUMBER
7. AUTHOR(s) D. A. MacLanahan, Jr. - ARO, Inc.		8. CONTRACT OR GRANT NUMBER(s)
9 PERFORMING ORGANIZATION NAME AND ADDRESS Arnold Engineering Development Center, Arnold Air Force Station, Tennessee 37389		10 PROGRAM ELEMENT, PROJECT, TASK AREA & WORK UNIT NUMBERS Program Element 64733 Project Number 1906-00
11 CONTROLLING OFFICE NAME AND ADDRESS Armament Development Test Center (SDTT) Eglin Air Force Base, Florida 32542		12. REPORT DATE February 1975
		13. NUMBER OF PAGES 39
14 MONITORING AGENCY NAME & ADDRESS(if different from Controlling Office)		15 SECURITY CLASS (of this report) UNCLASSIFIED
		15a. DECLASSIFICATION/DOWNGRADING SCHEDULE N/A

16 DISTRIBUTION STATEMENT (of this Report)

Distribution limited to U.S. Government agencies only; this report contains information on test and evaluation of military hardware; February 1975; other requests for this document must be referred to Armament Development Test Center (SDTT), Eglin Air Force Base, Florida 32542.

17 DISTRIBUTION STATEMENT (of the abstract entered in Block 20, if different from Report)

18 SUPPLEMENTARY NOTES

Available in DDC

19 KEY WORDS (Continue on reverse side if necessary and identify by block number)

Modular-Guided Glide Bomb	sensor systems
transonic flow	wind tunnels
aerodynamic systems	calibration
detectors	

20 ABSTRACT (Continue on reverse side if necessary and identify by block number)

Wind tunnel tests were conducted at Mach numbers from 0.50 to 1.50 to provide a calibration of the MGGB-II aerodynamic sensor systems and to determine the calibration sensitivity of these sensor systems to flight test hardware. Data indicated that, in addition to bench test calibrations for the sensors, aerodynamic calibrations are required to provide a complete sensor calibration package.

DD FORM 1473 EDITION OF 1 NOV 65 IS OBSOLETE
1 JAN 73

PREFACE

The work reported herein was conducted by the Arnold Engineering Development Center (AEDC), Air Force Systems Command (AFSC), at the request of the Armament Development Test Center (ADTC/SDTT), AFSC, under Program Element 64733, Project No. 1906-00 , for Celesco Industries. The results were obtained by ARO, Inc. (a subsidiary of Sverdrup & Parcel and Associates, Inc.), contract operator of AEDC, AFSC, Arnold Air Force Station, Tennessee. The work was done under ARO Project No. P41T-62A. Data reduction was completed on November 14, 1974. and the manuscript (ARO Control No. ARO-PWT-TR-74-125) was submitted for publication on December 16, 1974.

CONTENTS

ILLUSTRATIONS

1.0 INTRODUCTION

The modular-guided glide bomb (MGGB-II) is a high-speed air-launched gliding weapon system. After release from the parent aircraft, the wings are deployed to provide the desired lift. Vehicle attitude and motion requirements are established by an angle-of-attack sensing system and a pressure sensing system.

This test was conducted at Mach numbers from 0.50 to 1.50 to calibrate the MGGB-II aerodynamic sensor systems and to determine the calibration sensitivity of these sensor systems to flight test hardware.

2.0 APPARATUS

2.1 TEST FACILITY

Tunnel 16T is a closed-circuit, continuous-flow tunnel that can be operated at Mach numbers from 0.20 to 1.60. The test section is 16 by 16 ft in cross section and is 40 ft long. The tunnel can be operated within a stagnation pressure range from 80 to 4000 psfa, depending on the Mach number. Perforated test section walls allow continuous operation through the Mach number range with a minimum of wall interference. The location of the model in the test section is shown in Fig. 1. Additional information on the tunnel, its capability, and the available supporting equipment may be found in Ref. 1.

2.2 TEST ARTICLE

The model is a full-scale MGGB-II vehicle with the tail section removed and the wing span reduced to facilitate sting mounting and to prevent model loads from exceeding the allowable sting load capacity. The MGGB-II vehicle is a standard MK-82 bomb with a hemispherical nose section containing the guidance equipment and a strongback section which contains the wings and launch lugs. An installation photograph is presented in Fig. 2. A dimensional sketch of the model is shown in Fig. 3.

The alpha-beta (α-β) boom is equipped with two identical vane-type sensors that were mounted orthogonally to each other on the boom. A photograph and a dimensional sketch of the α-β boom are shown in Figs. 4 and 5, respectively. Each vane has a wedge-shaped section attached to a shaft which was attached to a pivot, thereby allowing the vanes to remain aligned with the local airflow. A pitot-static probe was an integral part of the nose of the boom.

A canard, mounted on the bottom of the guidance section, was equipped with a pitot-static probe for this test. There was also another vane-type sensor mounted on the left side of the model and two static pressure orifices, one each on the left and right sides. A photograph showing the canard, body-mounted vane-type sensor, and one of the pressure orifices is shown in Fig. 6. A dimensional sketch of the canard and the body-mounted angle-of-attack sensor is presented in Figs. 7 and 8, respectively.

2.3 INSTRUMENTATION

Four externally mounted strain gages were affixed to the sting to obtain data to correct the model angles due to sting deflections caused by aerodynamic loads. There were seven model-mounted pressure transducers which were used to measure the pressures on the alpha-beta boom pitot-static probe, the canard pitot-static probe, two body surface static orifices, and the pressure difference on the canard pitot-static probe. Electrical signals from the sting-mounted moment strain gages, pressure transducers, and model angle-of-attack and sideslip systems were digitized and recorded on magnetic tape as well as fed directly into a computer for on-line data reduction.

3.0 TEST DESCRIPTION

3.1 TEST PROCEDURE

Data were obtained by setting the appropriate tunnel conditions and taking steady-state data over the desired angle range. Combinations of angle-of-attack and sideslip were obtained by pitching and rolling the model. The pitch range was from -16 to 16 deg, and the sideslip range was from -10 to 10 deg at constant angles of attack of 0, 5, -10, and -15 deg. A summary of test conditions is presented in Table 1.

3.2 DATA REDUCTION

Sting strain-gage readings were used to calculate forces and moments. These, in turn, were used to determine the corrections which were applied to the model angles of attack and sideslip to account for sting deflections.

3.3 DATA UNCERTAINTIES

Uncertainties (bands which included 95 percent of the calibration data) of the basic tunnel parameters (PT_∞, TT, and M_∞) were estimated from calibrations of the instrumentation and from the repeatability and uniformity of the test-section flow during tunnel calibrations. These estimates were used to determine uncertainties of other free-stream properties using the Taylor series method of error propagation. Additional information concerning the uncertainties in the free-stream properties is discussed in Refs. 2 and 3.

6

Where sting deflections are needed to define the angles of attack and sideslip, the uncertainty in angle of attack and sideslip is ±0.25 deg. However, when the model-mounted angular position indicator was used to define the angles of attack and sideslip, the uncertainty is ±0.1 deg. The model-mounted indicator was used at model roll angles of 0, 180, and 90 deg.

The estimated uncertainties are given below:

M_∞	ΔM_∞	Δq_∞, psf	ΔCP
0.7	±0.0020	±1.2	±0.015
0.9	±0.0026	±1.0	±0.015
1.3	±0.0100	±1.2	±0.014
1.5	±0.0128	±1.1	±0.014

4.0 RESULTS AND DISCUSSION

4.1 ANGLE-OF-ATTACK AND SIDESLIP SENSORS

Calibration data for both of the angle-of-attack sensors and the sideslip angle sensor are presented in Figs. 9 through 12. All of these data show good linearity. When compared with the body-mounted vane sensor, the alpha-beta boom sensors show better linearity with the slope more nearly equal to one. Upright and inverted data have the same slope with a small offset due to flow angularity. Subsonically, the zero offset for all three sensors agrees well. The zero offset is positive and less than one degree. Only at Mach number 1.00 is the zero offset on the boom angle-of-attack sensor greater than one degree. The zero offset on the boom angle-of-sideslip sensor is greater than one degree at Mach numbers 1.00 to 1.30. Since the zero offsets for all three sensors agree at the lower and higher Mach numbers, the disagreement near Mach number 1.00 is probably due to shock location on the model. Figure 10 shows the effect of angle of attack on the angle-of-sideslip sensor calibration. Increasing the angle of attack had no discernible effect on the slope but decreased the zero offset. The boom angle-of-attack sensor output for various sideslip angles (Fig. 11) shows good agreement with the calibration data presented in Fig. 9.

Figure 12 shows the effects of the presence of the alpha-beta boom and wing sweep on the angle of attack of the body-mounted sensor. These data show no influence due to wing sweep but the presence of the alpha-beta boom slightly increased the zero offset. These data, however, maintained good linearity.

4.2 PRESSURE SENSORS

Calibration data for both pitot-static probes and the two surface static pressure orifices are presented in Figs. 13 through 18. Within the test range, the total pressure, as measured by the pitot-static probe on the alpha-beta boom, was not appreciably influenced by angle of attack or angle of sideslip. The canard pitot pressure is influenced by both angle of attack and angle of sideslip. Subsonically, at high negative angles of attack (greater than -12 deg), the canard pitot pressure decreased with decreasing angle of attack. Supersonically, as the angle of attack was increased, the canard pitot pressure increased. As the absolute value of the angle of sideslip increased, the canard pitot pressure decreased. The canard pitot pressure is greatly influenced by wing sweep angle, particularly at supersonic speeds. Sweeping the wings aft decreased the canard pitot pressure.

Calibration data for the alpha-beta boom static and canard static pressures show the following: (1) the boom static pressure is not appreciably influenced by angle of attack but decreased as the absolute value of the angle of sideslip was increased, (2) generally, the canard static pressure increased as the angle of attack was increased, and the offset at $a_m = 0$ deg increased as the Mach number was increased, (3) the canard static pressure was not appreciably influenced by angle of sideslip, and (4) sweeping the wings aft decreased the canard static pressure but had negligible effect on the boom static pressure.

Left and right body surface static pressure data are presented in Figs. 17 and 18. Sweeping the wings aft, in general, decreased the surface static pressures. The right orifice is influenced more by sweeping the wings than the left orifice. The surface static pressures at $M_\infty = 0.95$ show an apparent effect of a normal shock in the vicinity of the orifices.
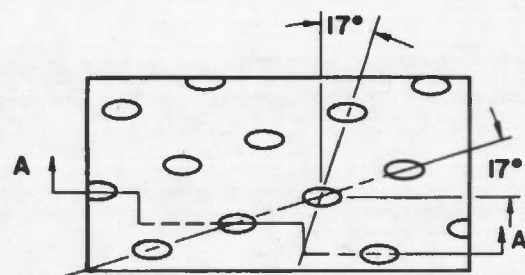
5.0 CONCLUSIONS

The results of the test conducted on two vane-type angle-of-attack sensors, one vane-type angle-of-sideslip sensor, two pitot-static probes, and two surface pressure orifices produced the following conclusions:

1. Generally, where comparisons were possible, the sensors on the alpha-beta boom produced more consistent results. The sensor data were not appreciably influenced by wing sweep or angle of attack. The probe static pressure was influenced only by angle of sideslip.

2. Both angle-of-attack sensors and the angle-of-sideslip sensor showed good linearity. For the test conditions, shock location had no appreciable effect on the angle sensors.
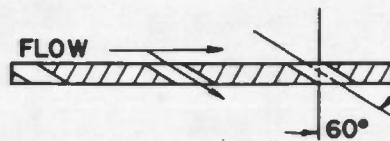
8

3. The pitot pressure on the alpha-beta boom was not appreciably influenced by angle of attack, angle of sideslip, or wing sweep. However, the pitot pressure on the canard was influenced by all three movements.

4. The probe static on the alpha-beta boom was influenced by angle of sideslip but not by angle of attack. The probe static on the canard was influenced by angle of attack but not by angle of sideslip.

REFERENCES

1. Test Facilities Handbook (Tenth Edition). "Propulsion Wind Tunnel Facility, Vol. 4." Arnold Engineering Development Center, May 1974.

2. Gunn, J. A. "Check Calibration of the AEDC 16-Ft Transonic Tunnel." AEDC-TR-66-80 (AD633277), May 1966.

3. Jackson, F. M. "Supplemental Calibration Results for the AEDC Propulsion Wind Tunnel (16T)." AEDC-TR-70-163 (AD872475), August 1970.

17°

FLOW

17°

17°

A

A

60°

Section A-A

6% Open Area
Hole Diameter = 0.75 In.
Plate Thickness = 0.75 In.
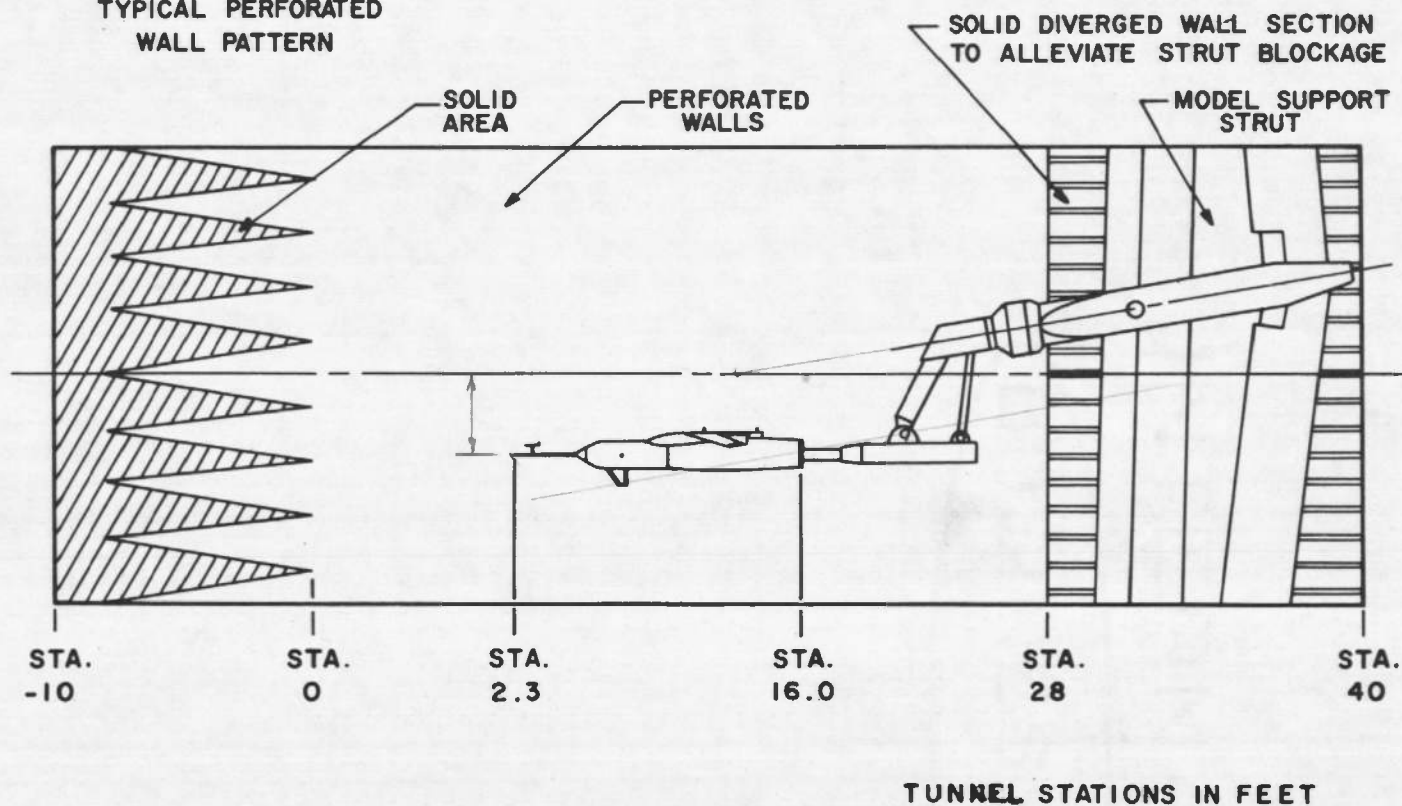
TYPICAL PERFORATED
WALL PATTERN

SOLID DIVERGED WALL SECTION
TO ALLEVIATE STRUT BLOCKAGE

SOLID
AREA

PERFORATED
WALLS

MODEL SUPPORT
STRUT

STA.
-10

STA.
0

STA.
2.3

STA.
16.0

STA.
28

STA.
40

TUNNEL STATIONS IN FEET

Figure 1. Sketch of model in 16T test section.

11

AEDC-TR-75-17
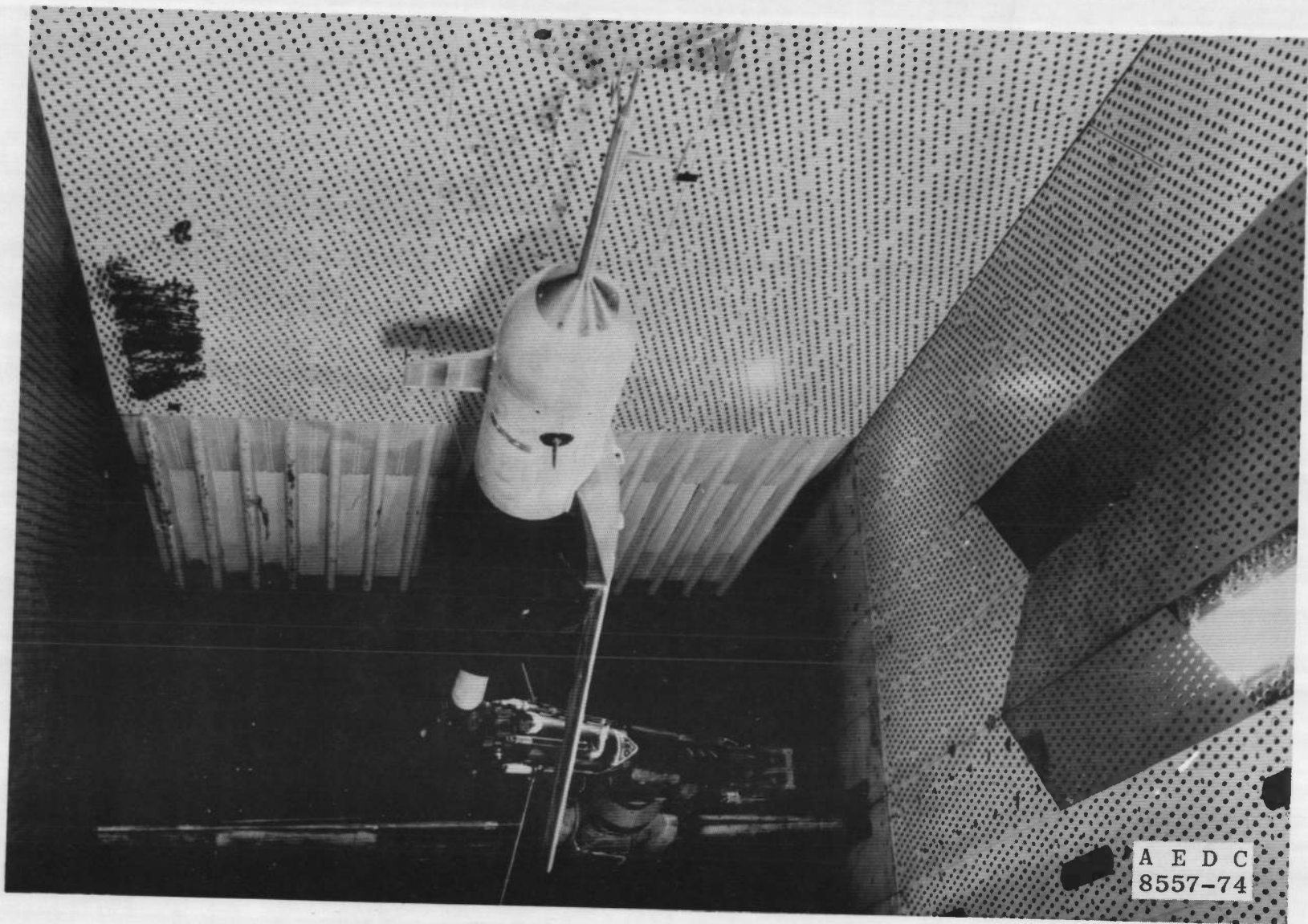
Figure 2. Installation photograph.
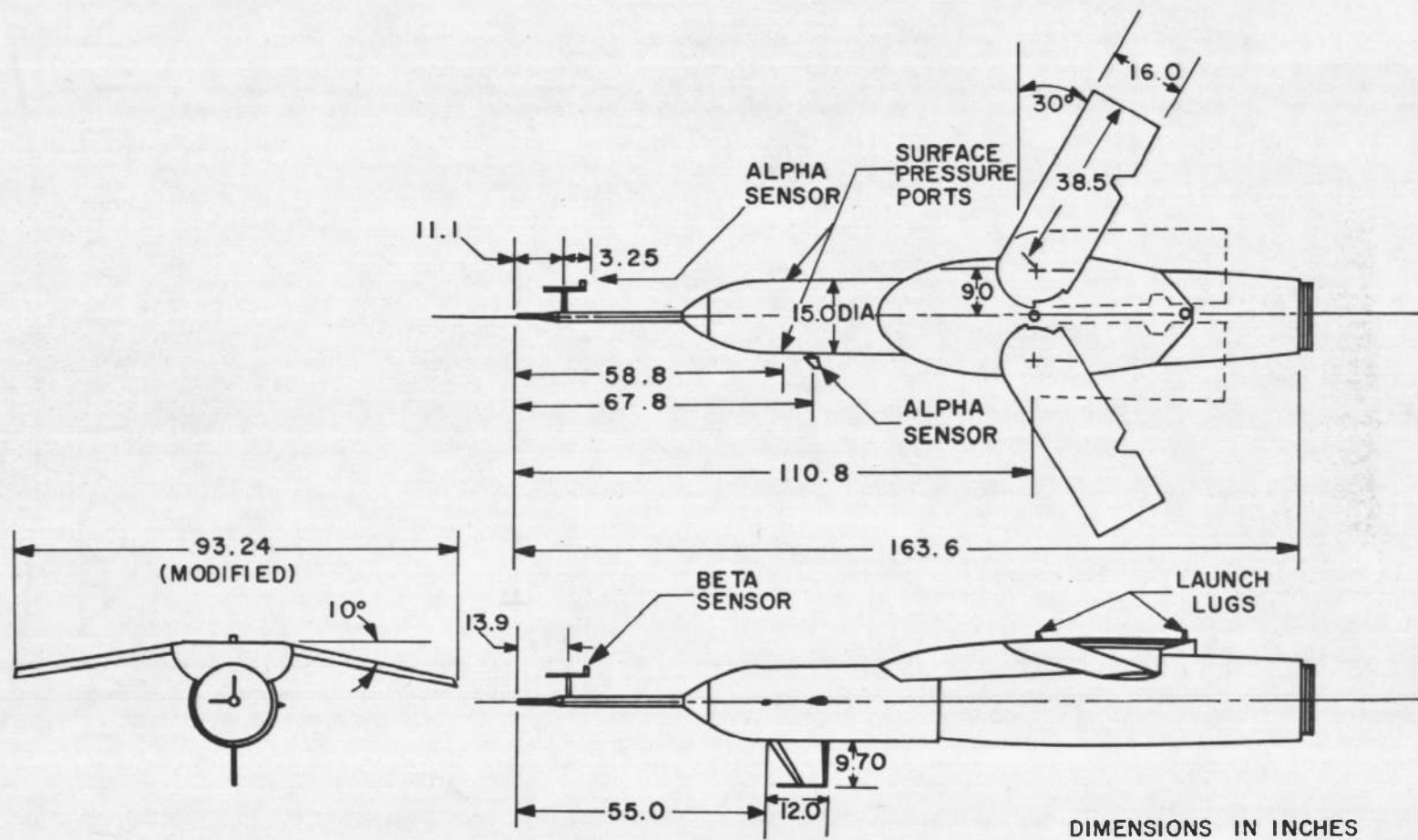
Figure 3. Dimensional sketch of model.
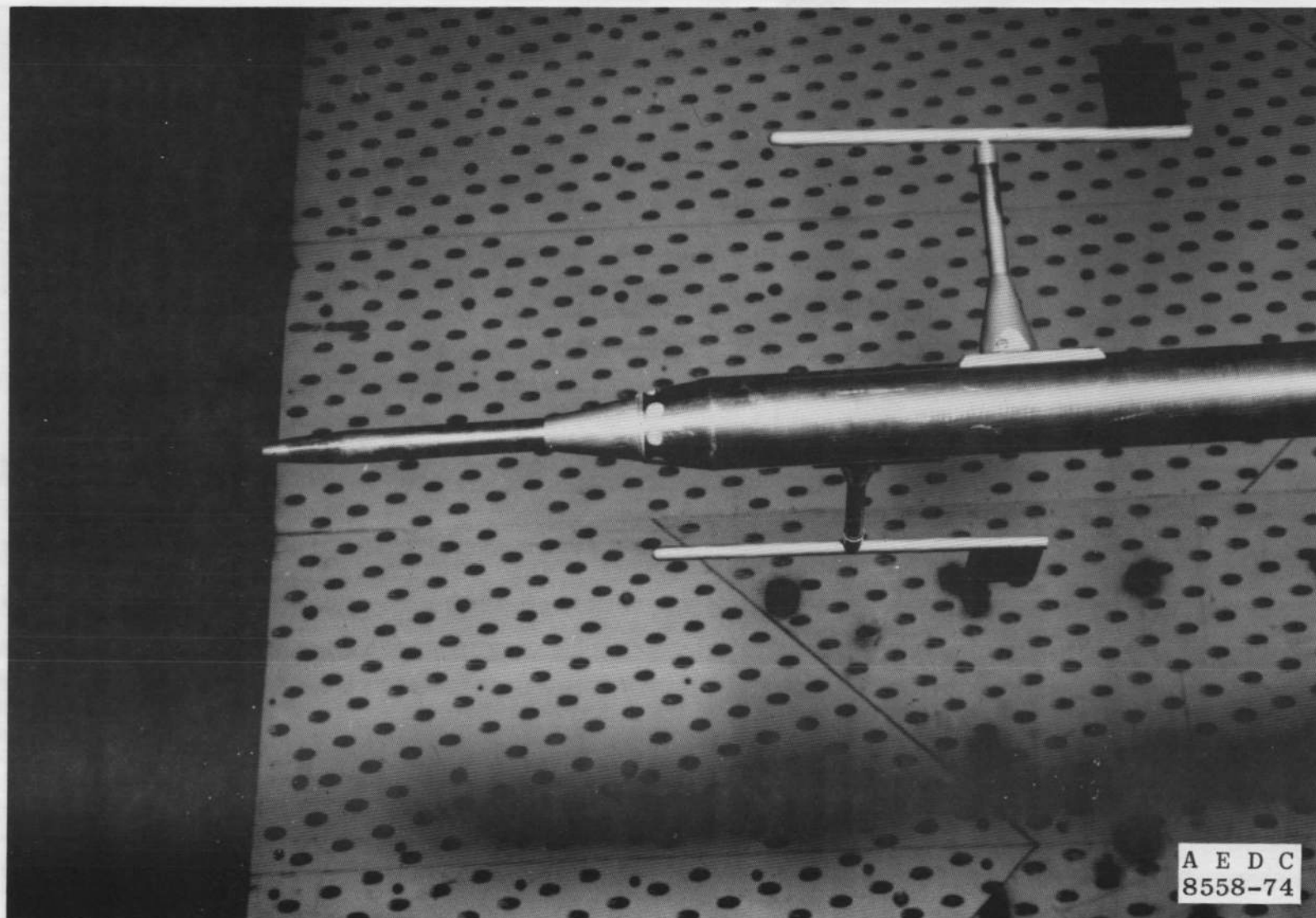
Figure 4. Photograph of alpha-beta boom sensor.

ALPHA
SENSOR

6.79

BETA
SENSOR

TOP VIEW

8.35

0.05

1.5

2.0

0.3 DIA

5.1

7.05

4.00

DIMENSIONS IN INCHES

PITOT-STATIC
PROBE

1.75 DIA.

8.84

5.44

35.35

RIGHT SIDE VIEW
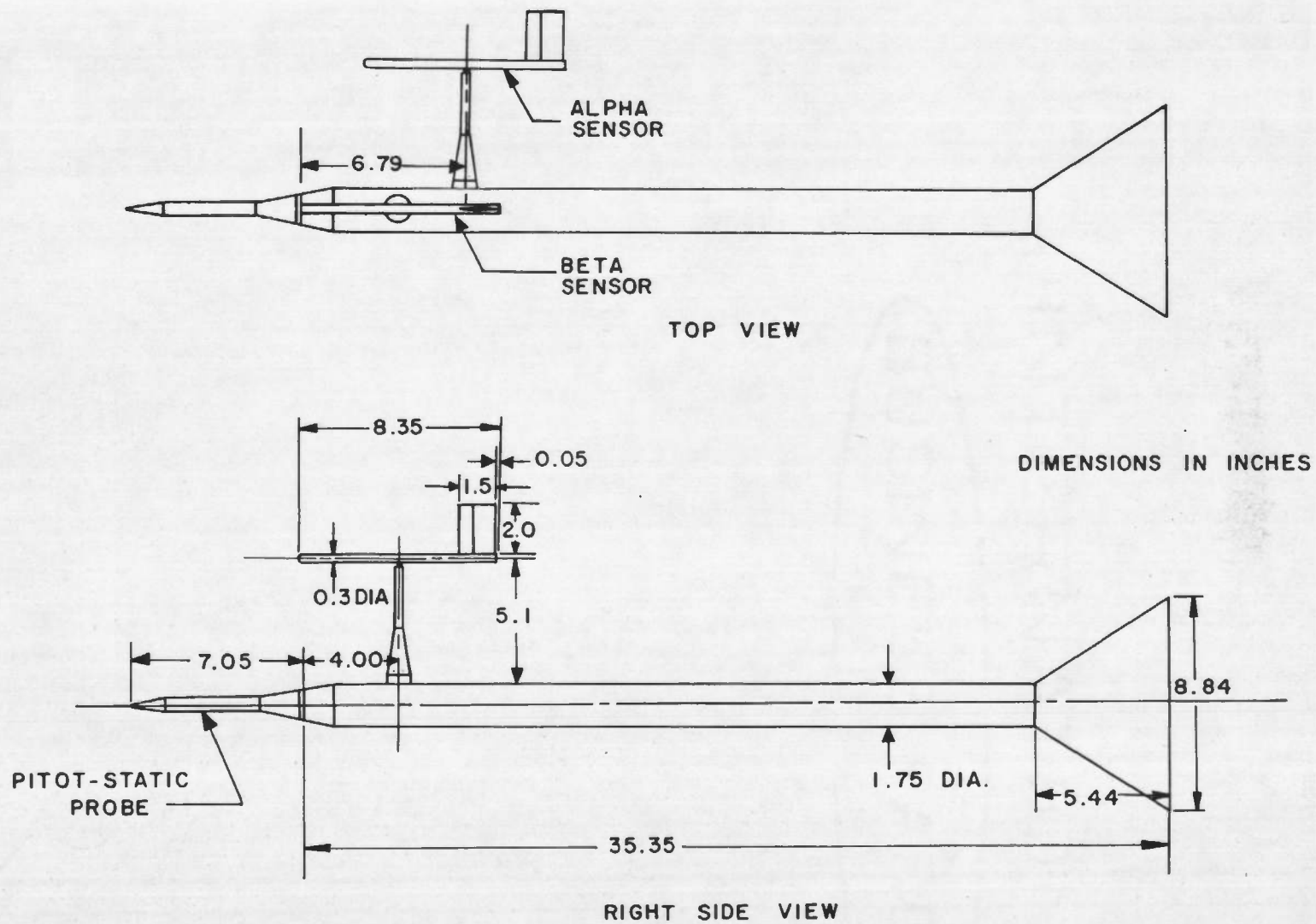
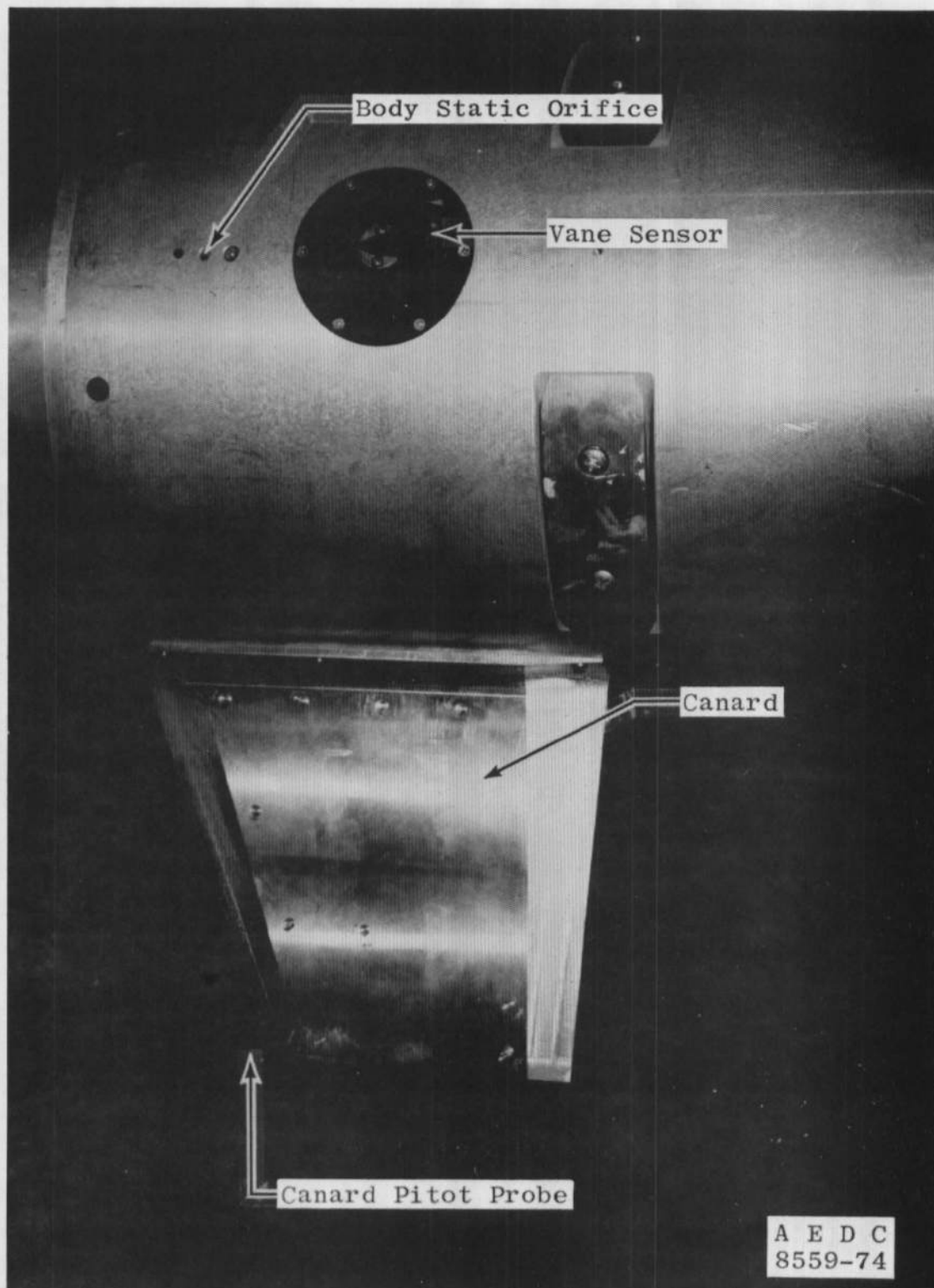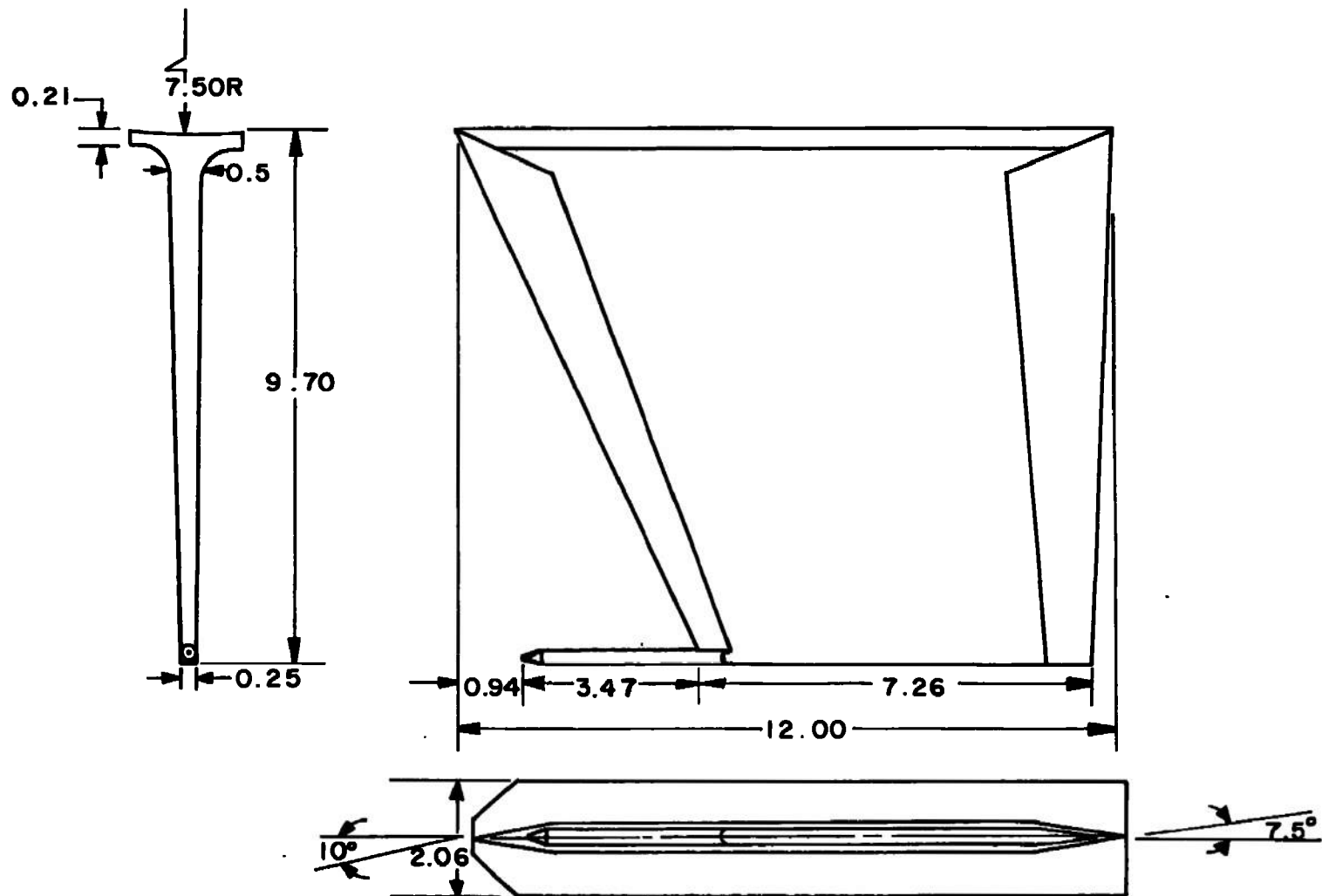Figure 5. Dimensional sketch of alpha-beta boom sensor.

15

AEDC-TR-75-17

Figure 6. Photograph of canard and body-mounted vane sensor.

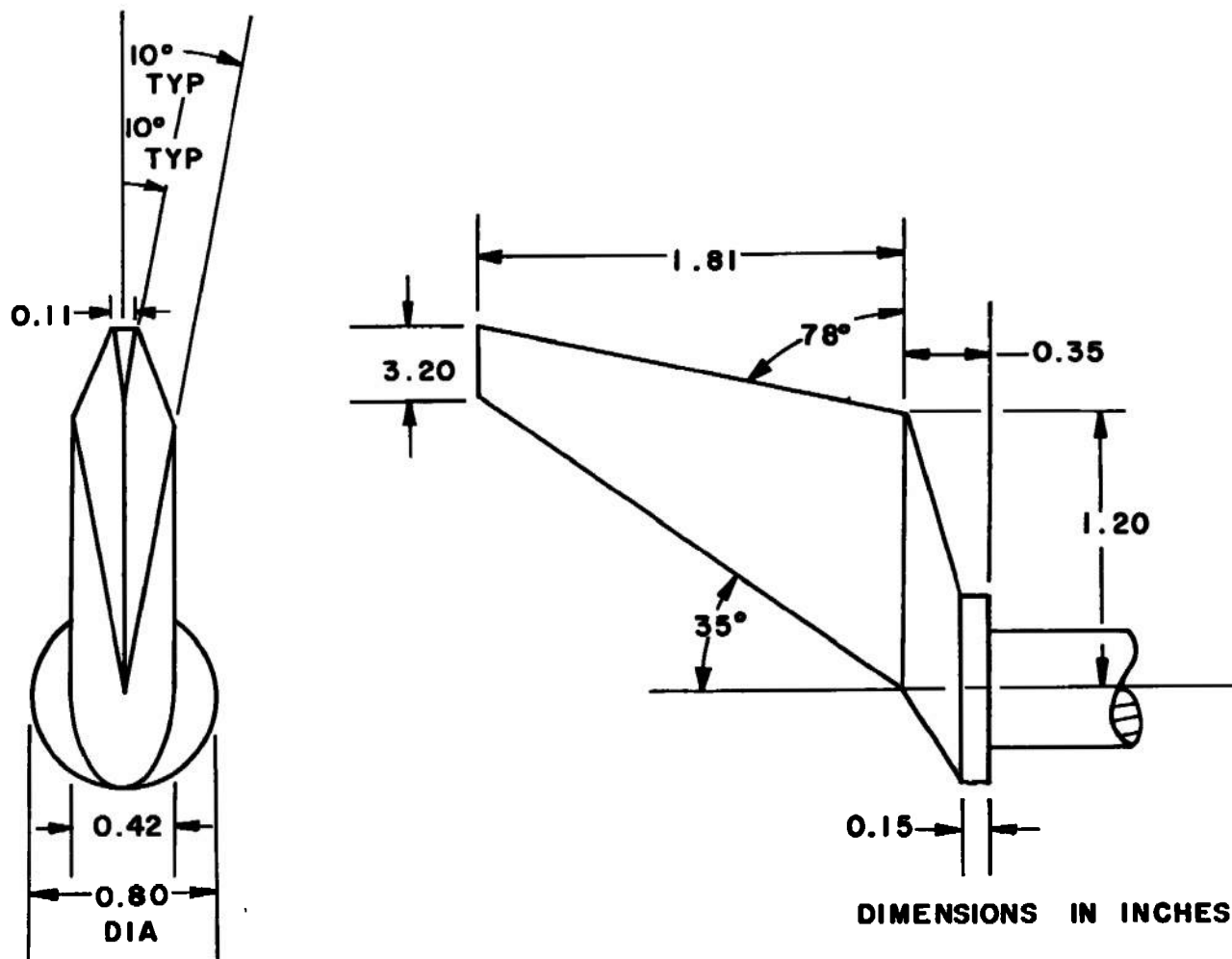DIMENSIONS IN INCHES

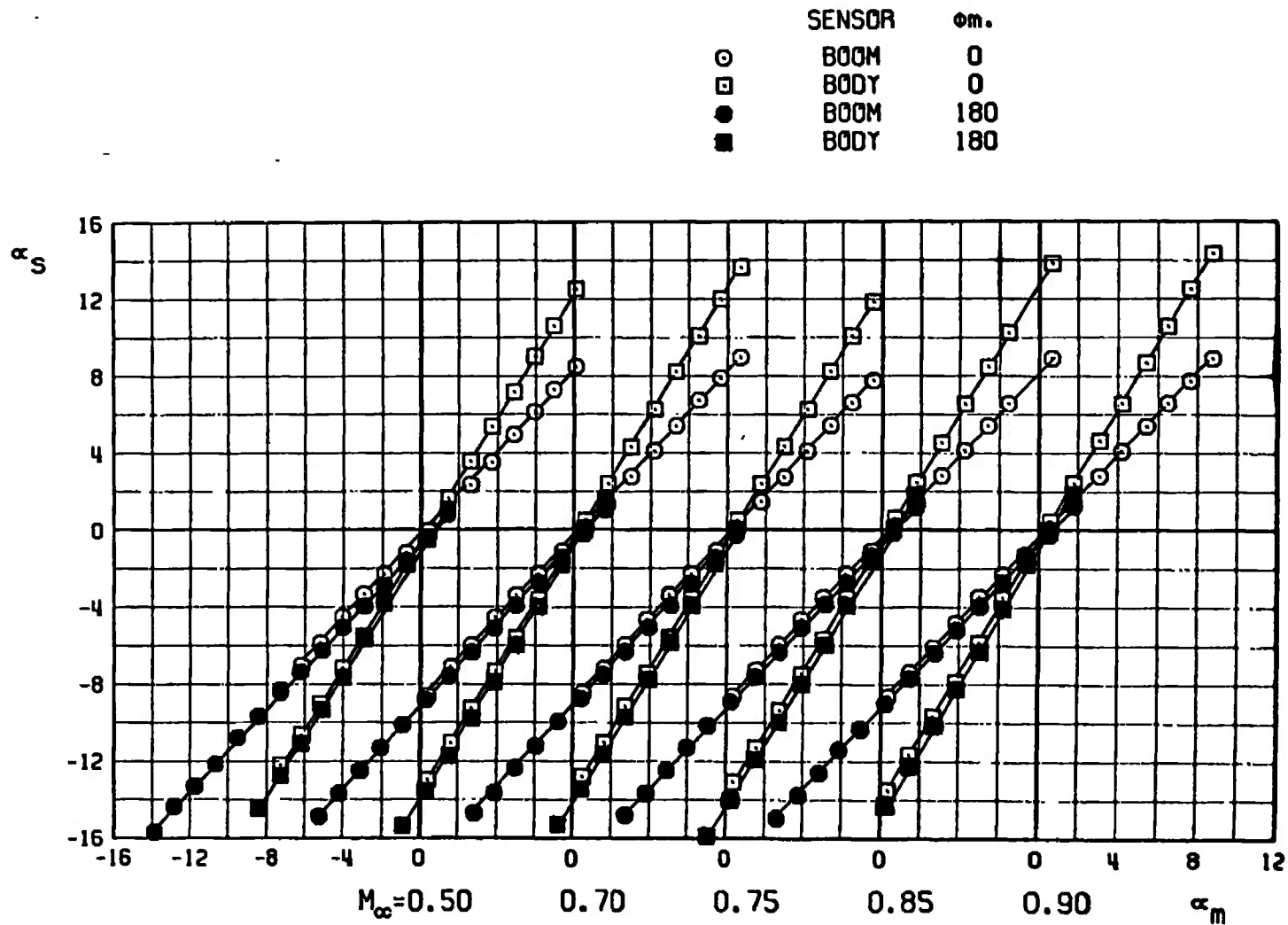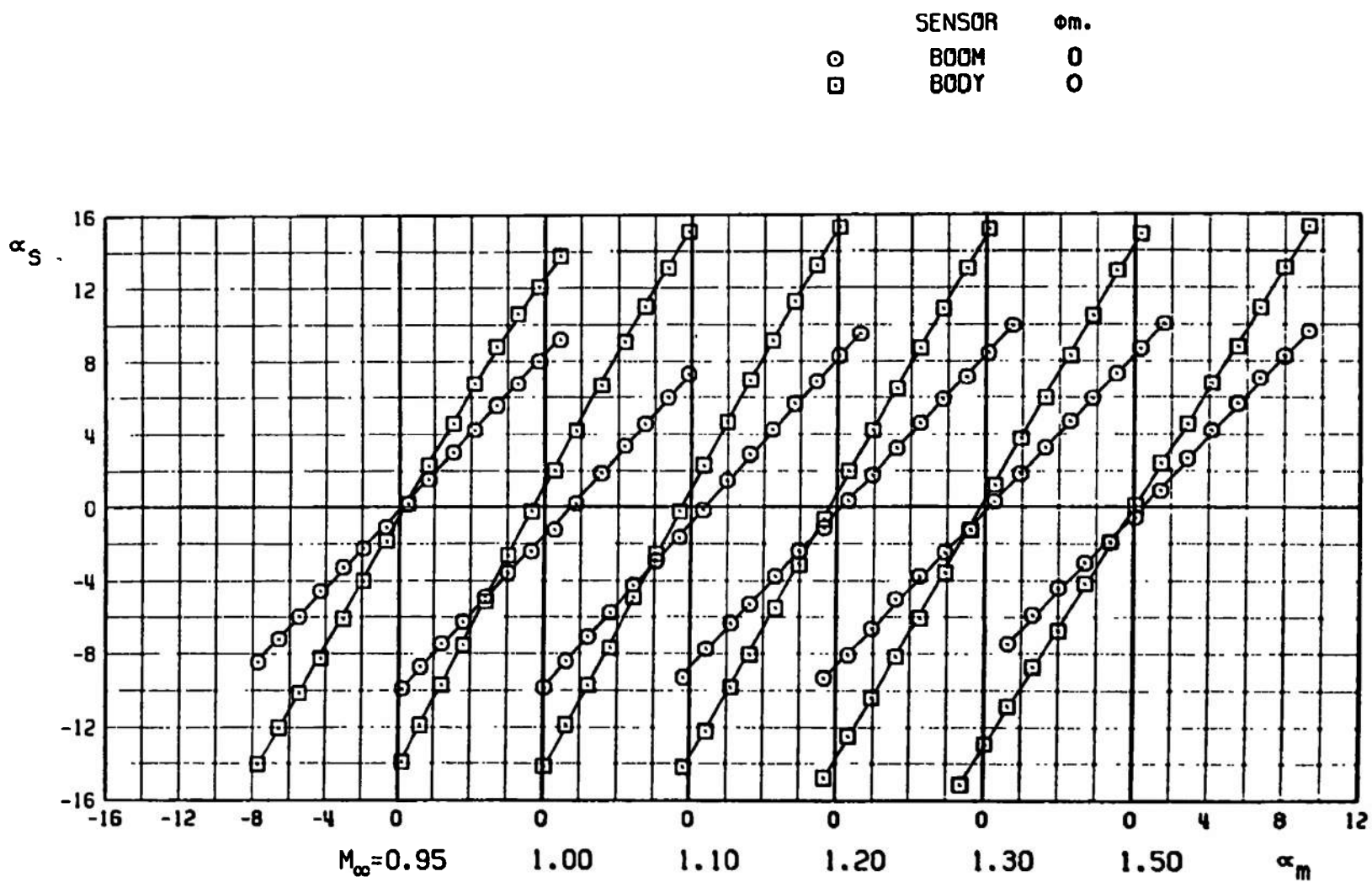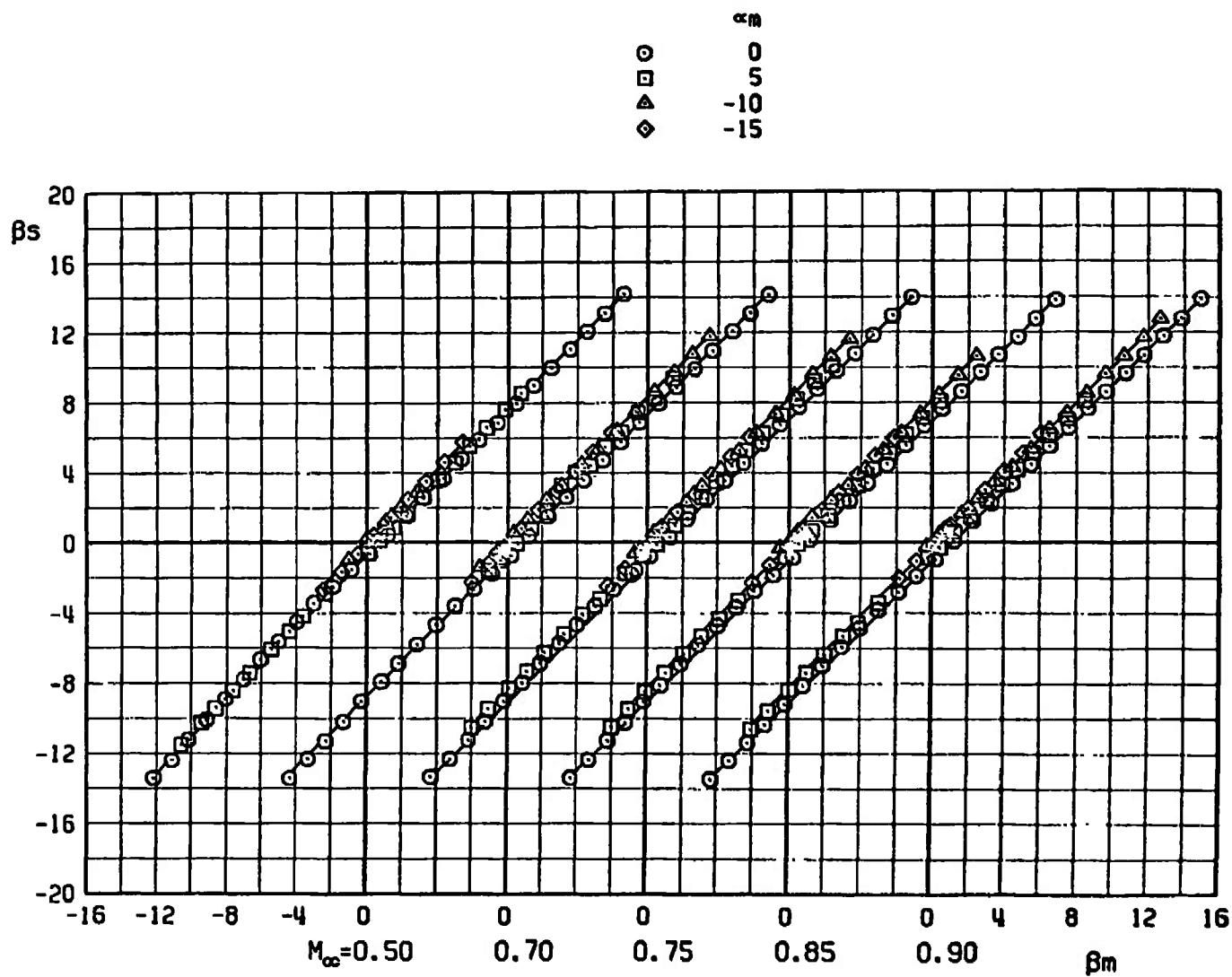Figure 7. Dimensional sketch of canard.

Figure 8. Dimensional sketch of body-mounted vane sensor.

a. Mach numbers 0.50 to 0.90

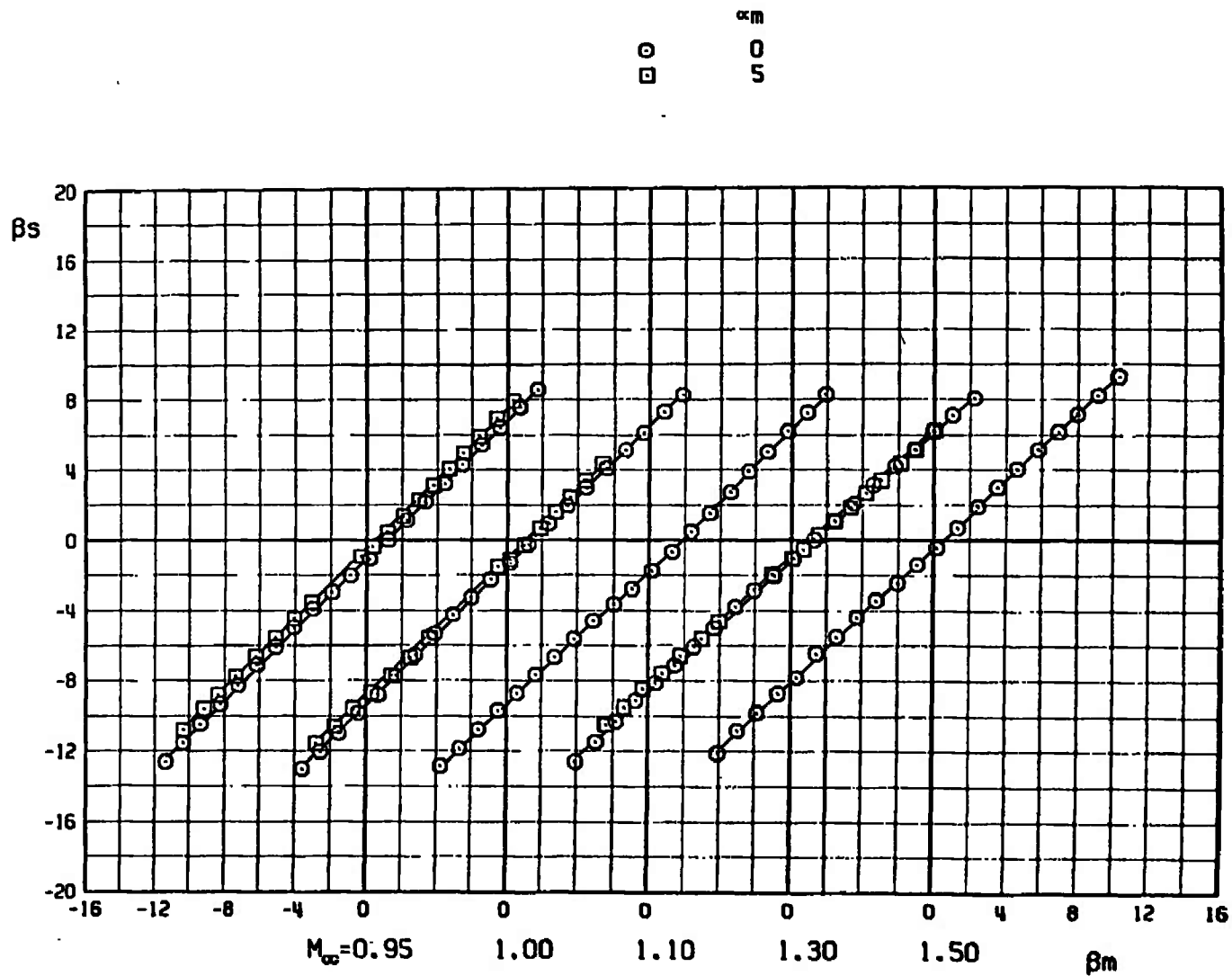Figure 9. Angle-of-attack calibration data, Λ_w = 30 deg.

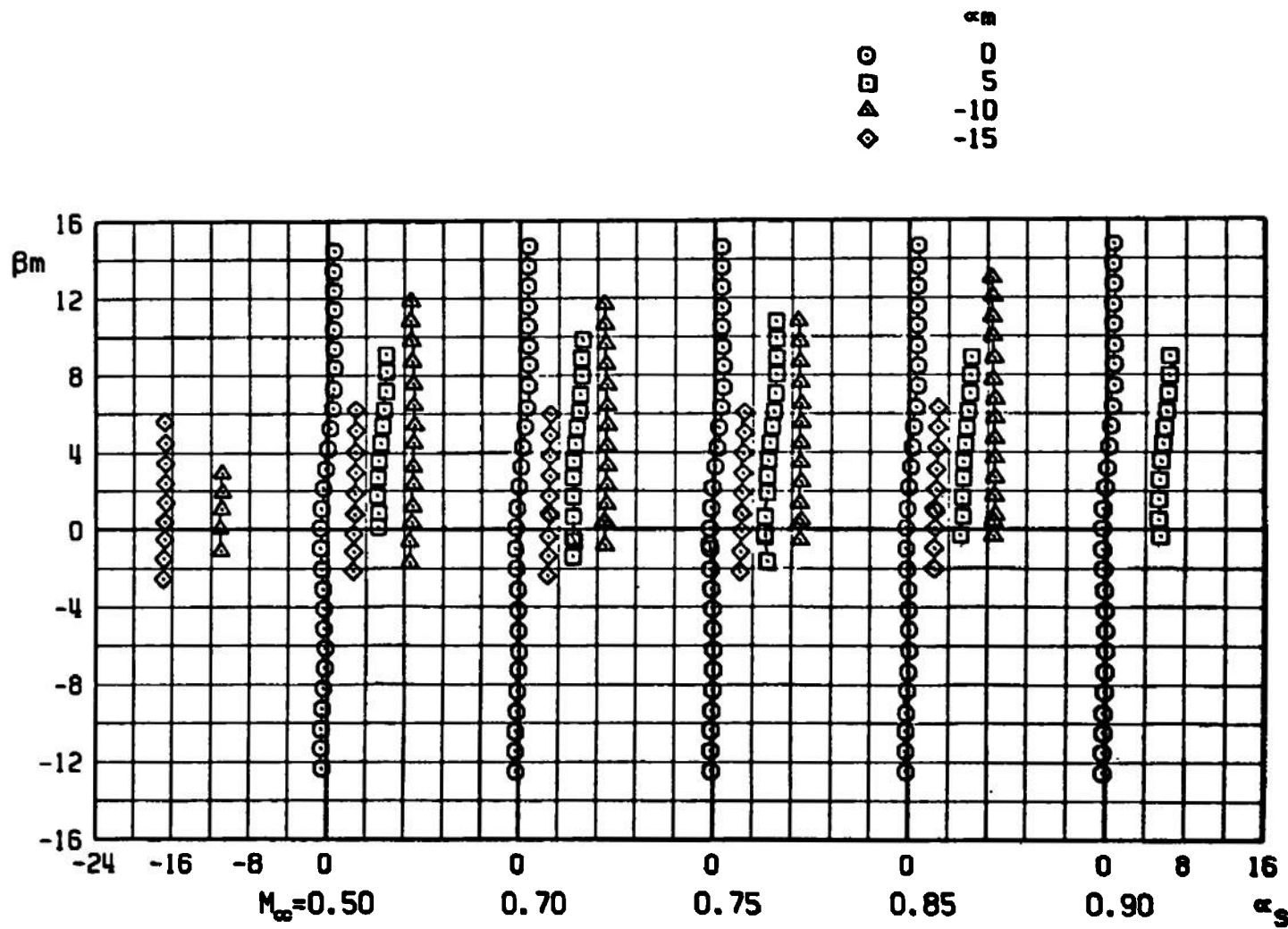b. Mach numbers 0.95 to 1.50
Figure 9. Concluded.

a. Mach numbers 0.50 to 0.90

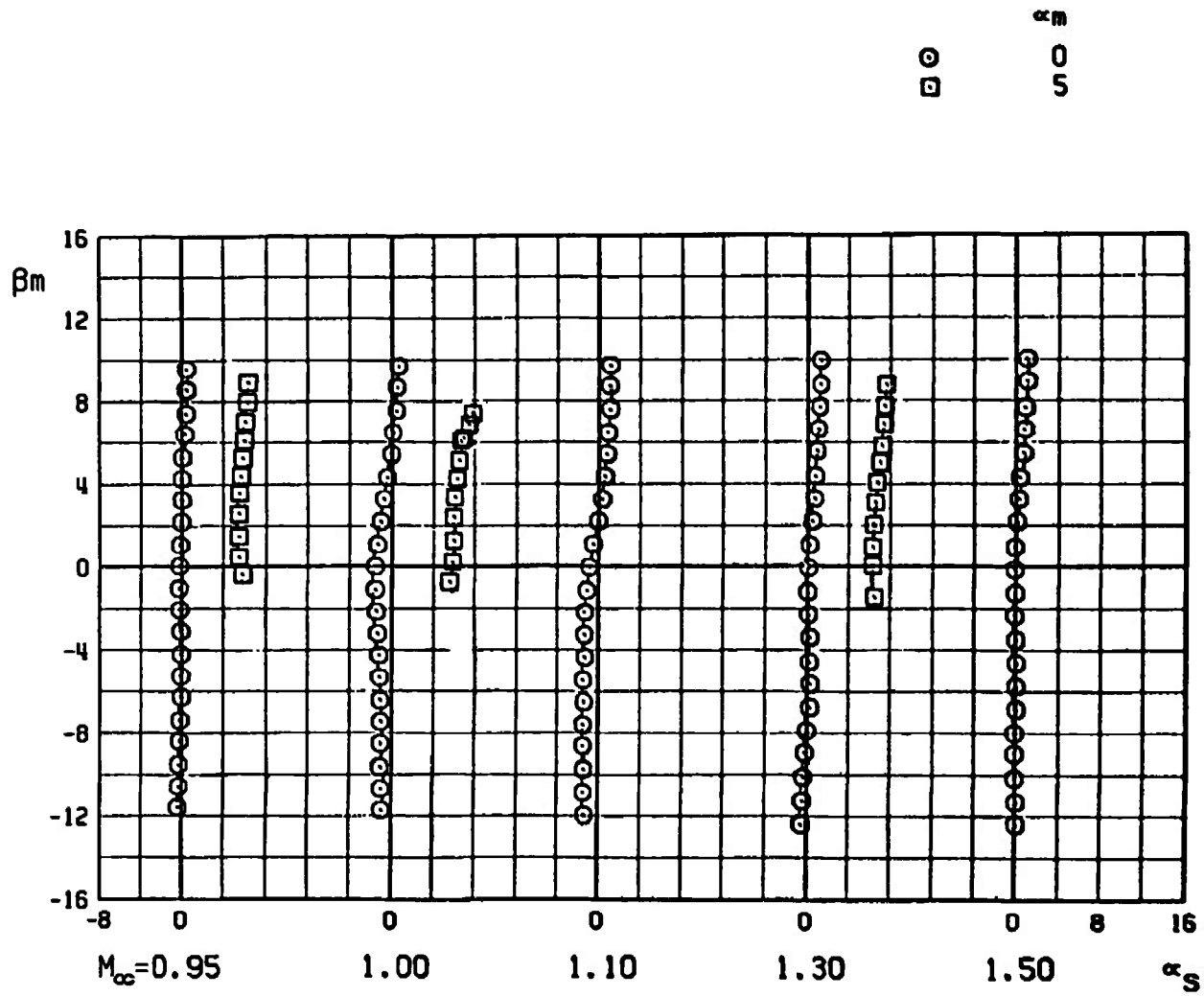Figure 10. Angle-of-sideslip calibration data, Λ_w = 30 deg.

b. Mach numbers 0.95 to 1.50
Figure 10. Concluded.

α_m

⊙   0
⊡   5
△   -10
◇   -15

β_m

16
12
8
4
0
-4
-8
-12
-16

-24   -16   -8   0   0   0   0   0   8   16

$M_\infty=0.50$ 0.70   0.75   0.85   0.90 α_s

a. Mach numbers 0.50 to 0.90

Figure 11. Effect of angle of sideslip on alpha-beta boom-mounted angle-of-attack
sensor, Λ_w = 30 deg.

b. Mach numbers 0.95 to 1.50
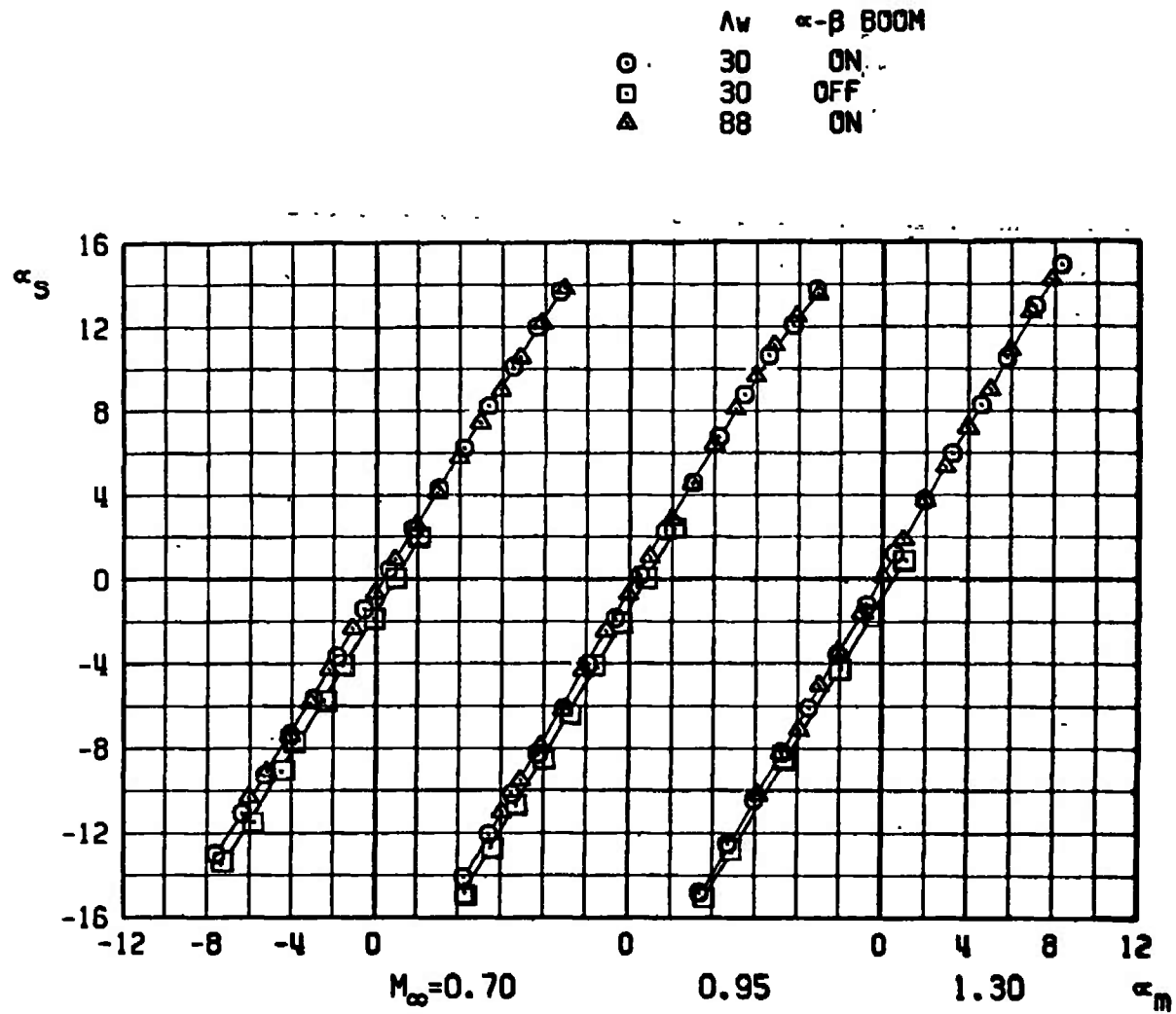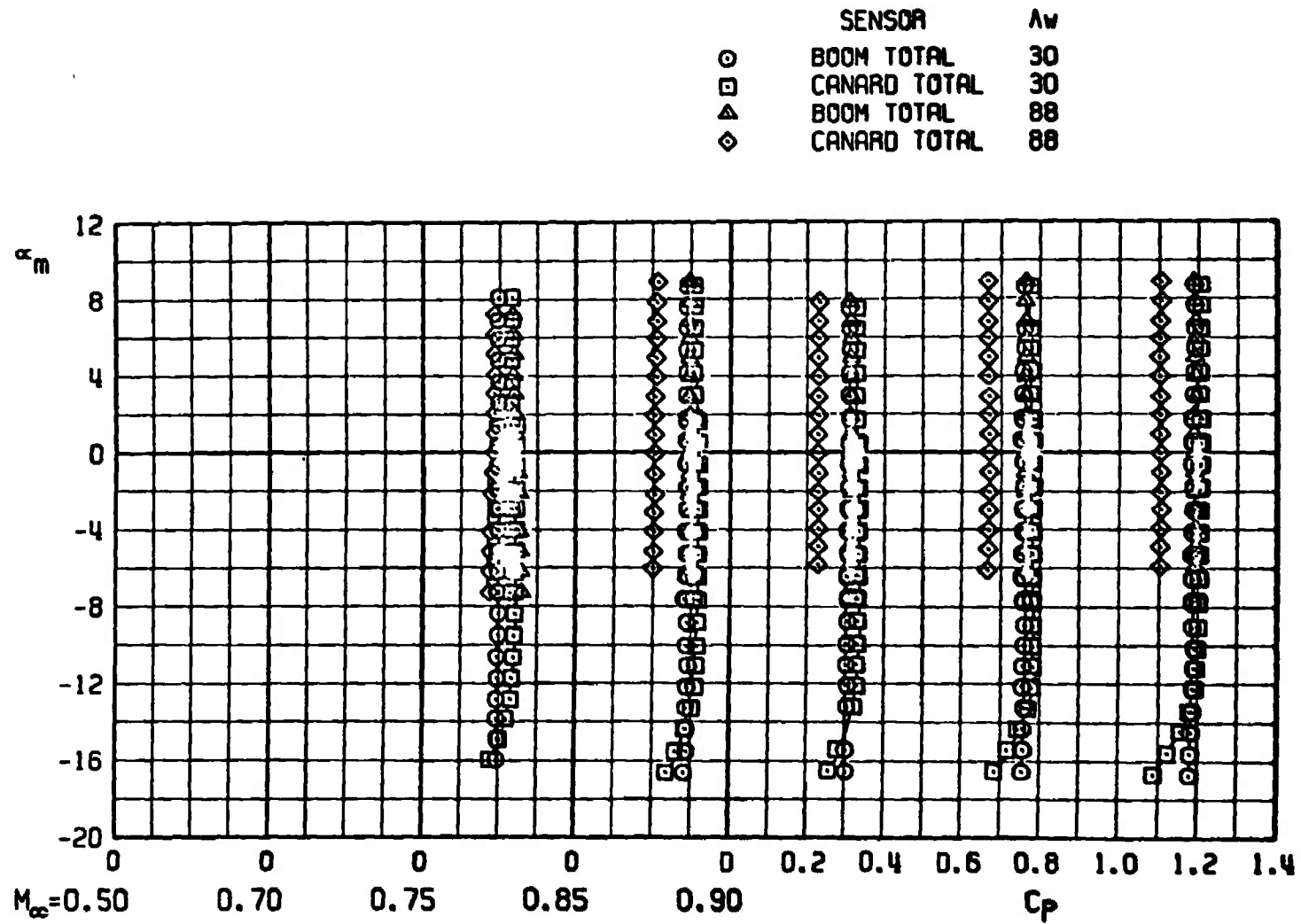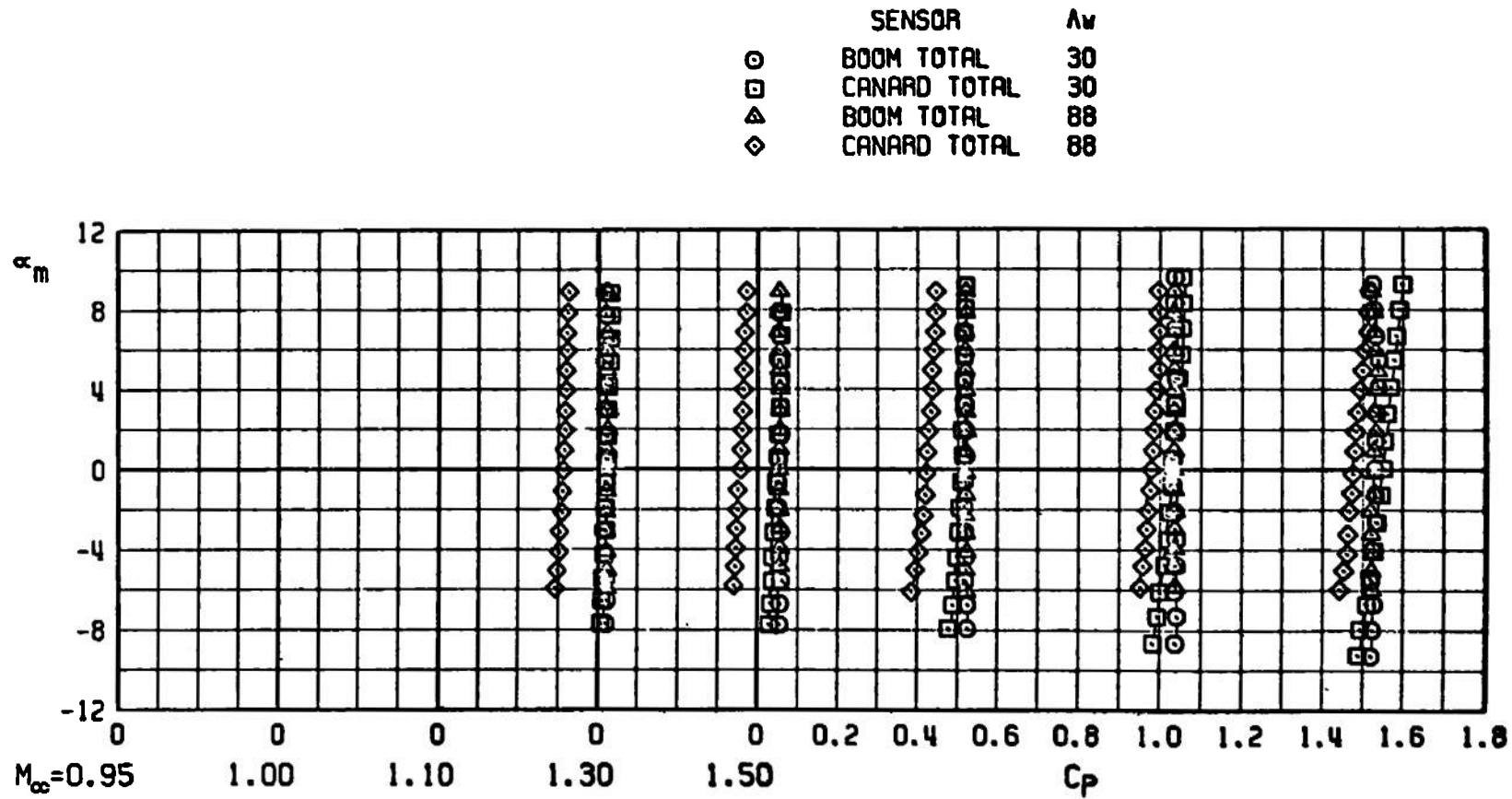Figure 11. Concluded.

Figure 12. Configuration effects on body-mounted vane sensor.

a. Mach numbers 0.50 to 0.90

Figure 13. Effect of angle of attack on total pressure sensors.

b. Mach numbers 0.95 to 1.50
Figure 13. Concluded.
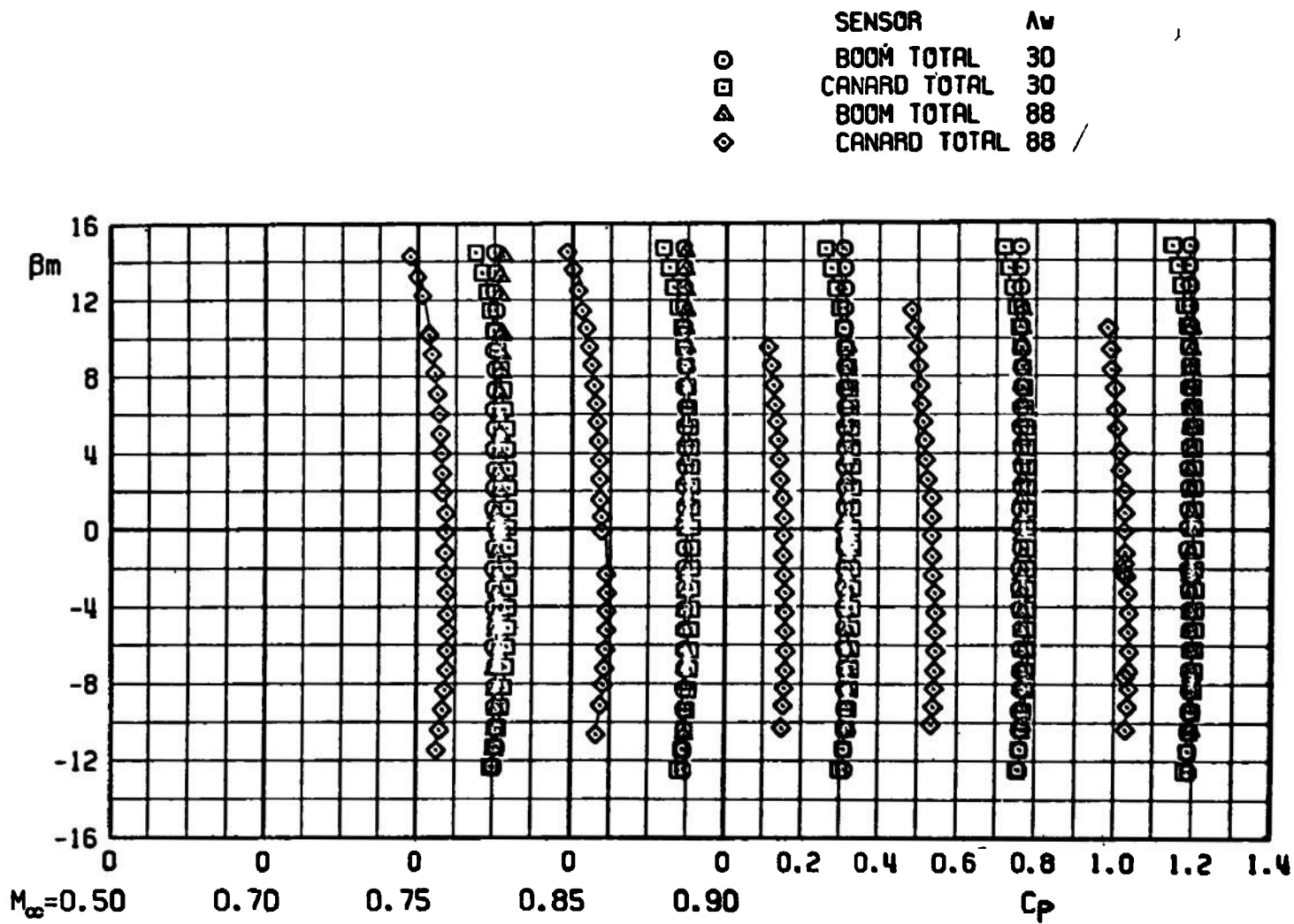
a. Mach numbers 0.50 to 0.90

Figure 14. Effect of angle of sideslip on total pressure sensors.

SENSOR   Λw

⊙   BOOM TOTAL   30
☐   CANARD TOTAL   30
△   BOOM TOTAL   88
◇   CANARD TOTAL   88

b. Mach numbers 0.95 to 1.50
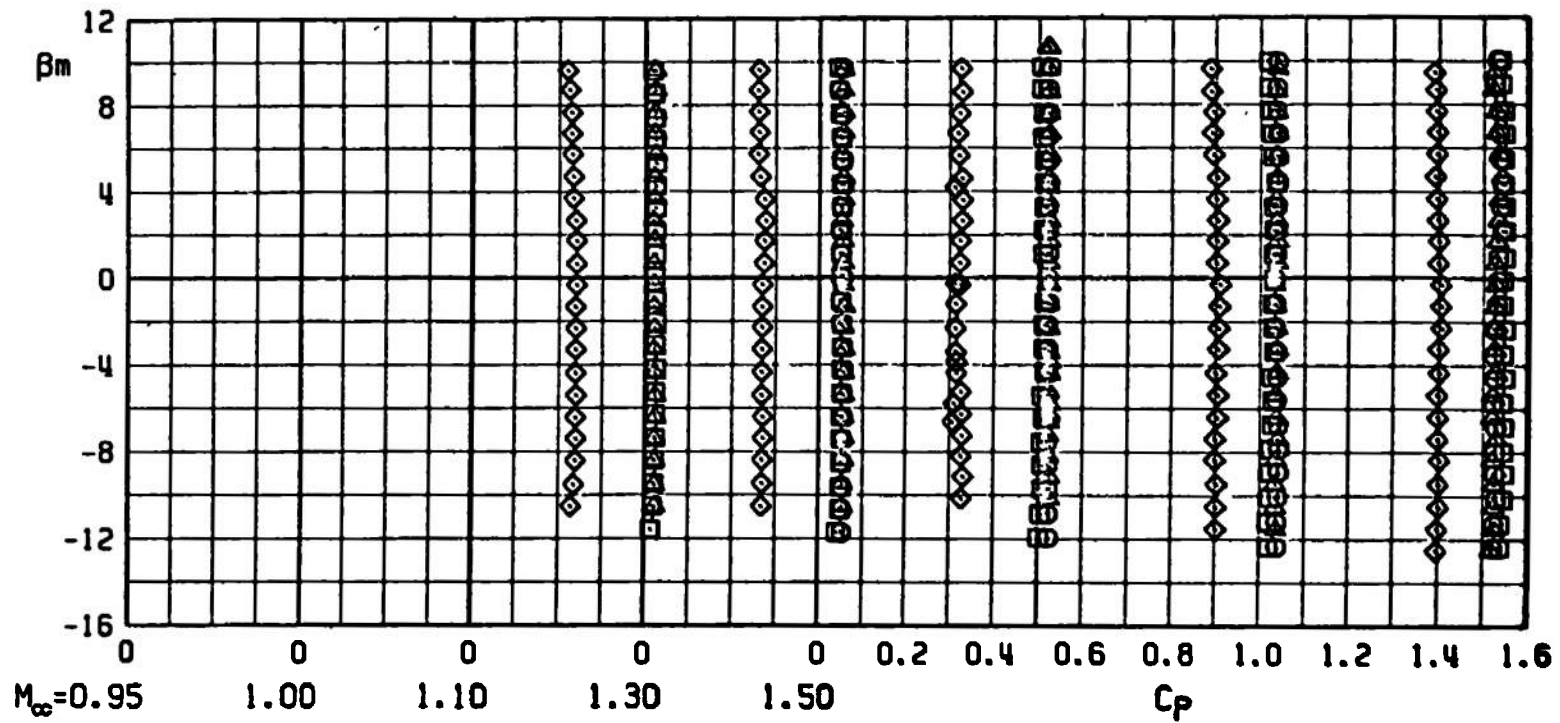Figure 14. Concluded.

a. Mach numbers 0.50 to 0.90.

Figure 15. Effect of angle of attack on probe static pressure sensors.

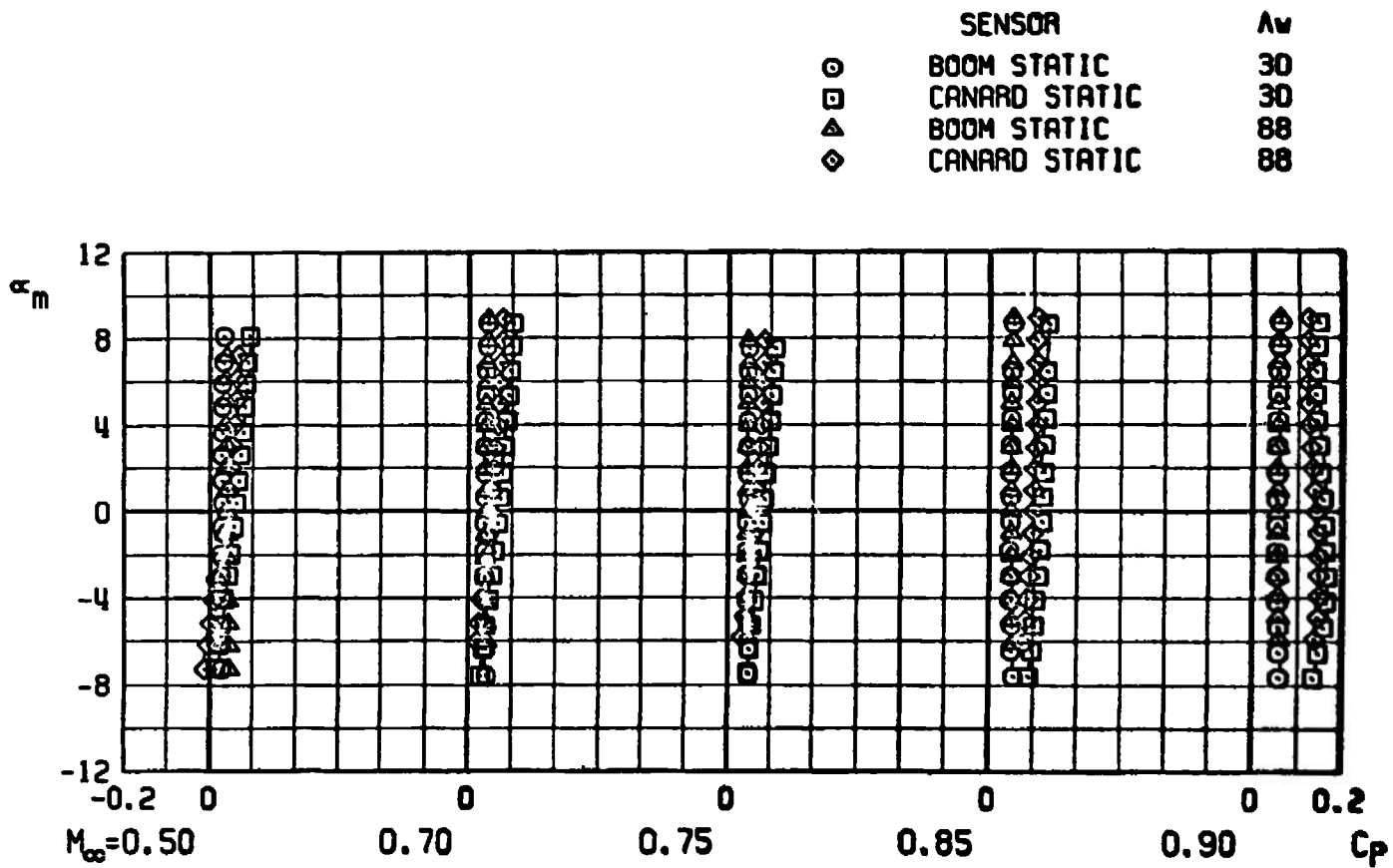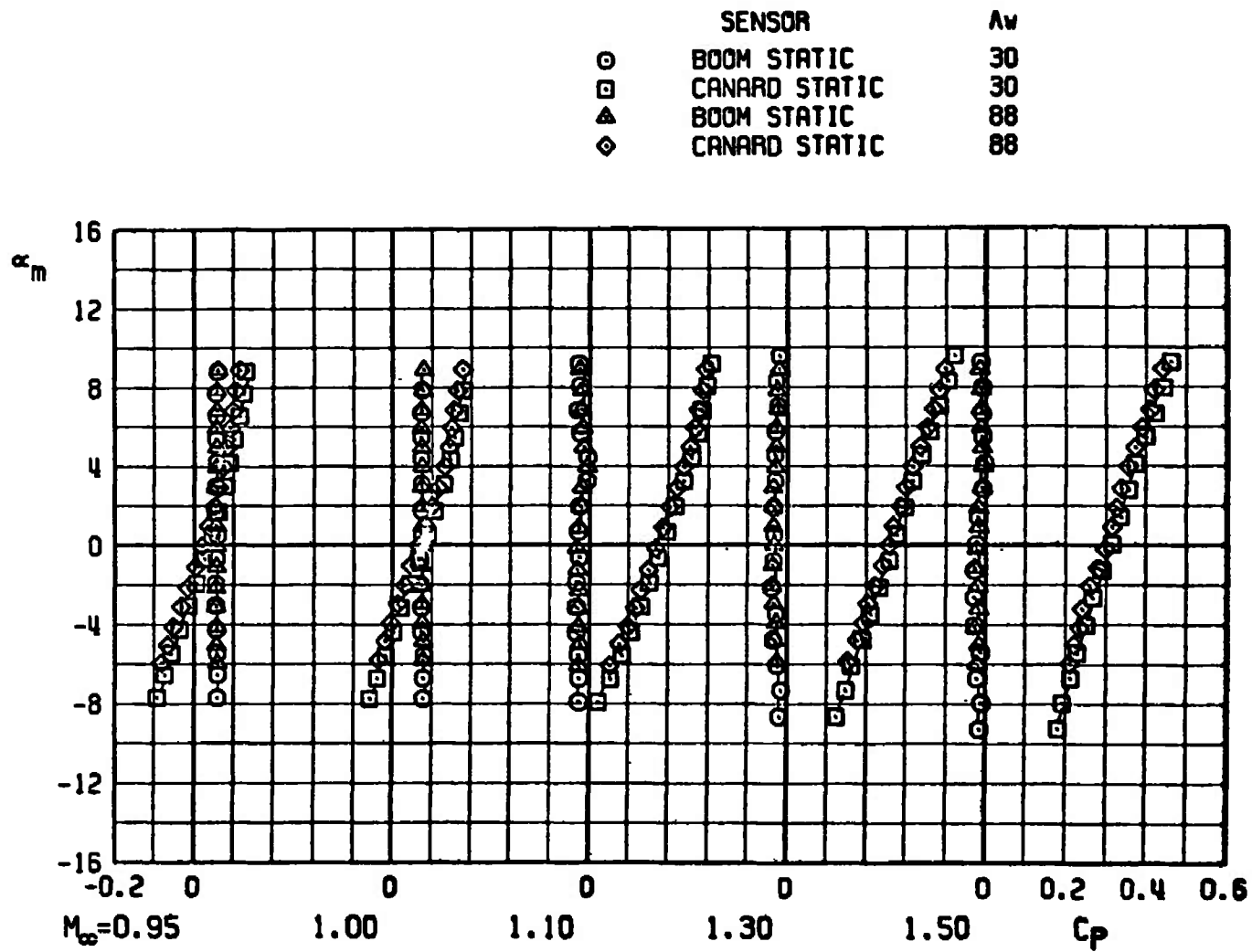b. Mach numbers 0.95 to 1.50
Figure 15. Concluded.

SENSOR		Λv
⊙	BOOM STATIC	30
⊡	CANARD STATIC	30
△	BOOM STATIC	88
◇	CANARD STATIC	88

βm

16

12

8

4

0

-4

-8

-12

-16

-0.4 -0.2   0   0   0   0   0   0.2 0.4

M_∞=0.50   0.70   0.75   0.85   0.90 C_p

a. Mach numbers 0.50 to 0.90

Figure 16. Effect of angle of sideslip on probe static pressure sensors.

	SENSOR	Aw
⊙	BOOM STATIC	30
⊡	CANARD STATIC	30
△	BOOM STATIC	88
◇	CANARD STATIC	88
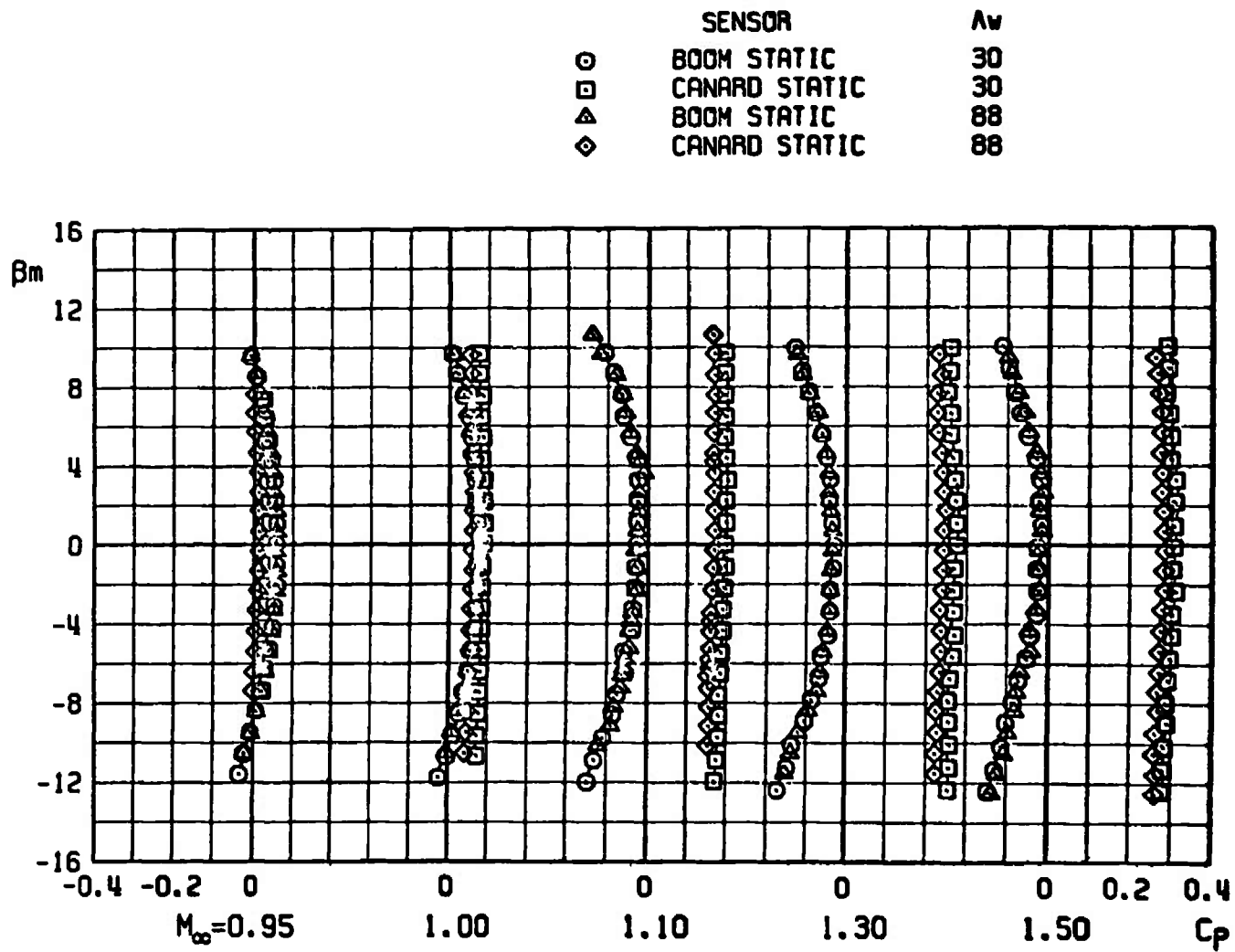
b. Mach numbers 0.95 to 1.50

Figure 16. Concluded.

33

AEDC-TR-75-17

a. Mach numbers 0.50 to 0.90

Figure 17. Effect of angle of attack on body surface static pressures.

SENSOR	Λw
⊙ LEFT BODY STATIC	30
⊡ RIGHT BODY STATIC	30
△ LEFT BODY STATIC	88
◇ RIGHT BODY STATIC	88
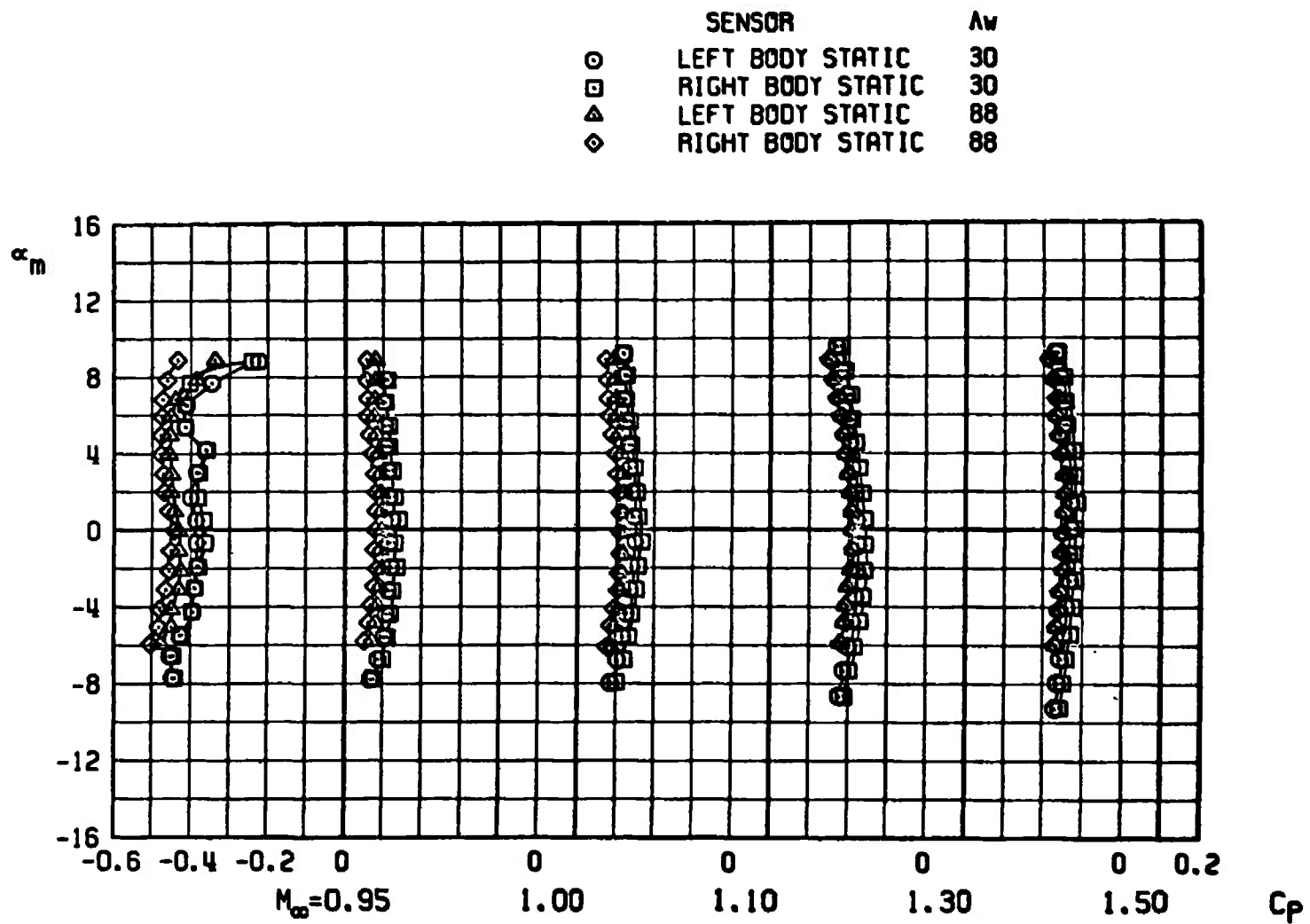
b. Mach numbers 0.95 to 1.50

Figure 17. Concluded.

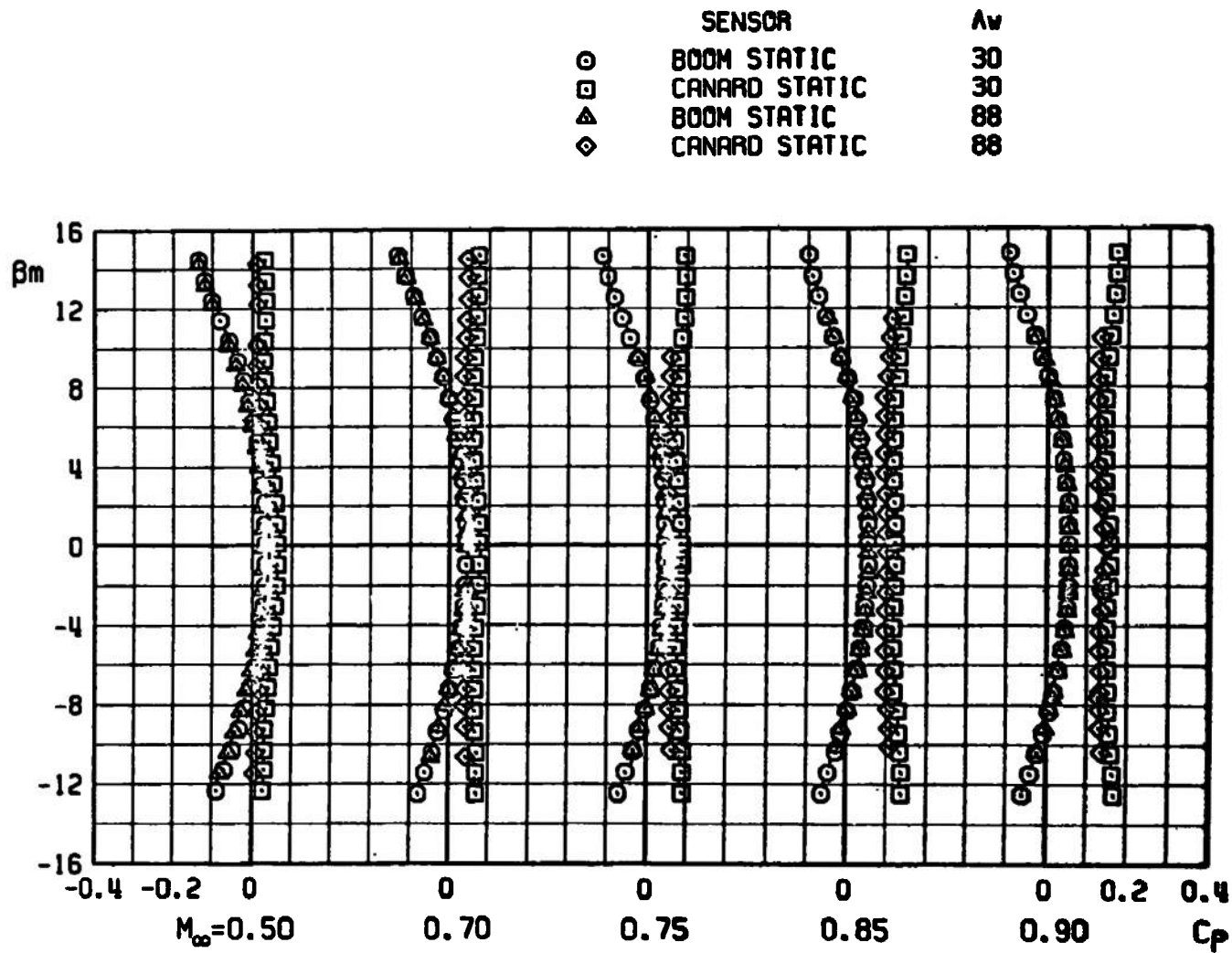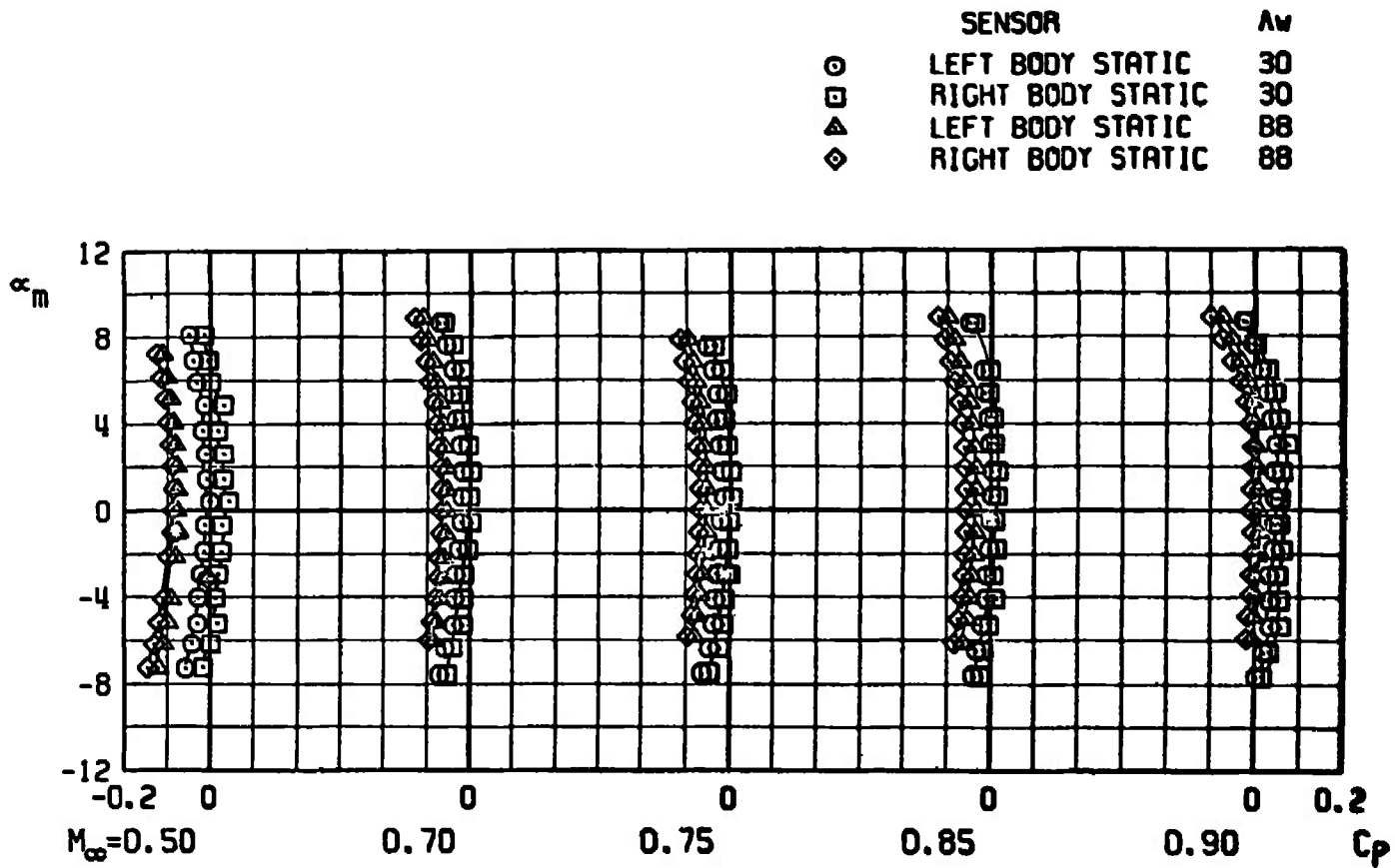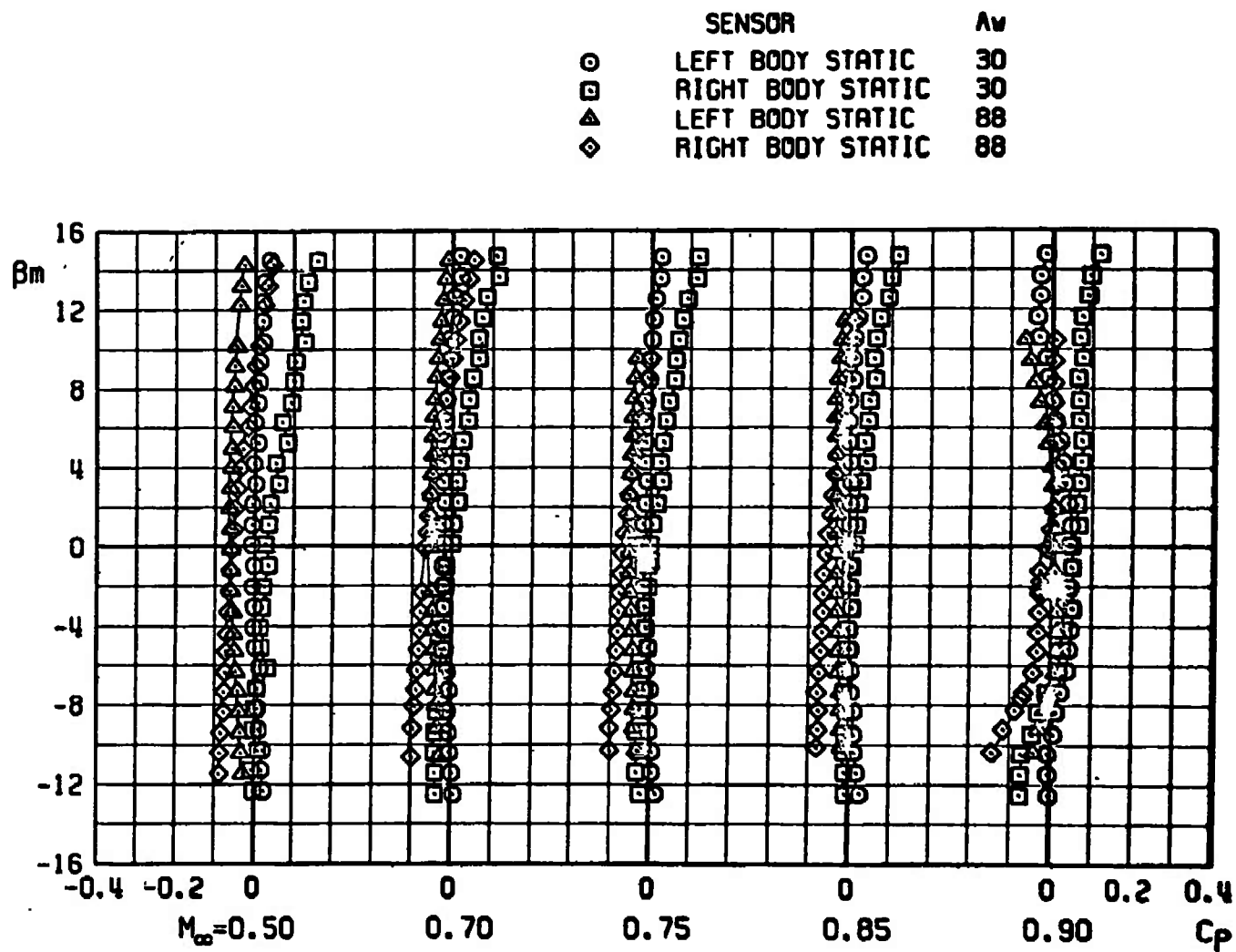|	SENSOR	Λv
⊙	LEFT BODY STATIC	30
⊡	RIGHT BODY STATIC	30
▲	LEFT BODY STATIC	88
◇	RIGHT BODY STATIC	88

a. Mach numbers 0.50 to 0.90

Figure 18. Effect of angle of sideslip on body surface static pressures.
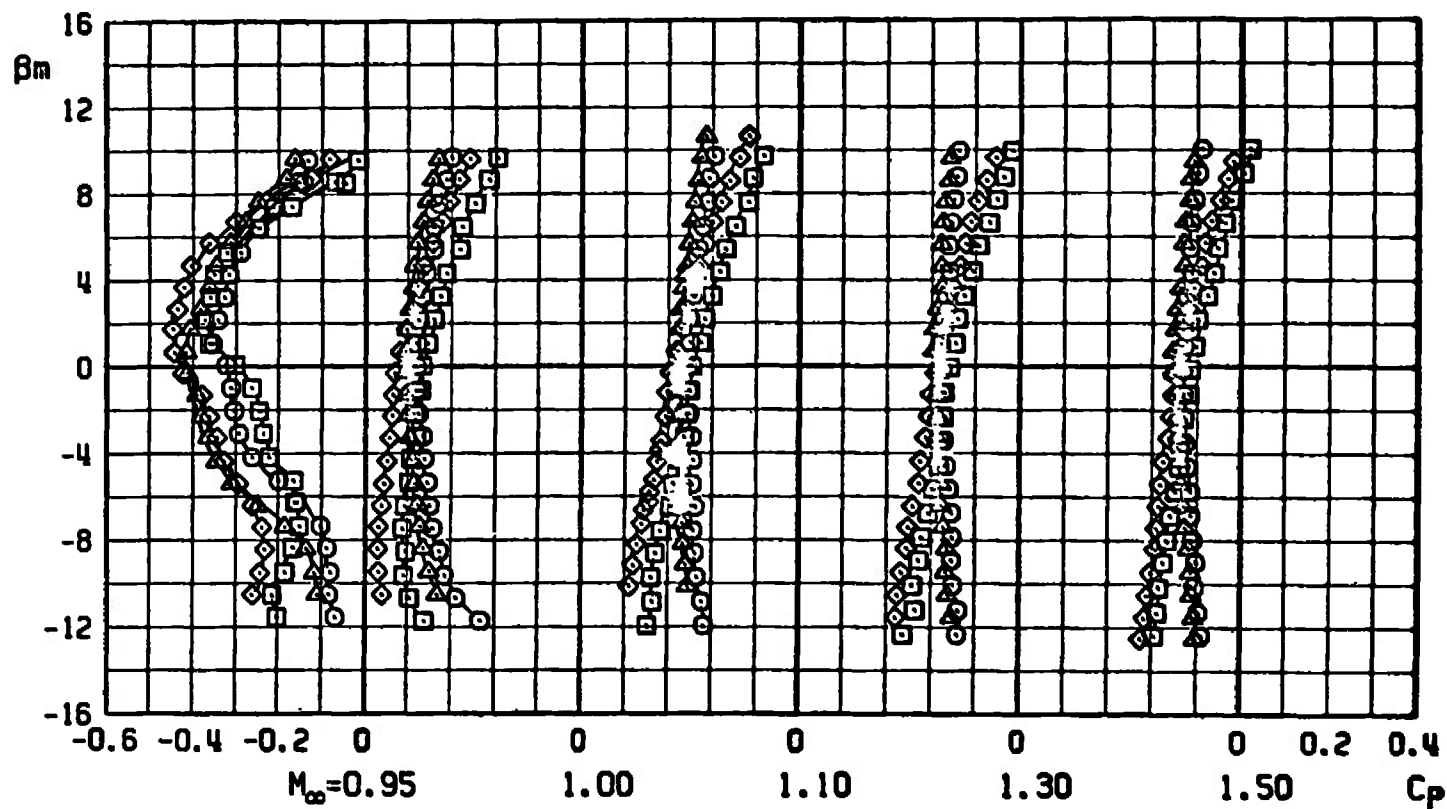
b. Mach numbers 0.95 to 1.50

Figure 18. Concluded.

Table 1. Summary of test conditions.

Configuration		Model Attitude			Mach Number and Total Pressure, psfa										
Boom	Λ_w, deg	α_m, deg	β_m, deg	ϕ_m, deg	0.50 1350	0.70 1200	0.75 1000	0.85 900	0.90 900	0.95 900	1.00 950	1.10 1000	1.20 1150	1.30 1300	1.50 1400
On	30	Var	0	0	17	20	25	26	31	32	35	36	38	39	42
		Var	0	180	18	22	23	28	29	--	--	--	--	--	--
		0	Var	90	19	21	24	27	30	33	34	37	--	40	41
		+5	Var	Var	86	69	74	75	78	81	83	84	--	85	--
		-10	Var	Var	87	70	73	76	79	--	--	--	--	--	--
		-15	Var	Var	88	71	72	77	80	--	--	--	--	--	--
On	88	Var	0	0	110	116	117	122	123	129	130	136	142	137	140
		0	Var	90	111	114, 115	118	121	124, 125	128	131	134	143, 144	138	141
		+5	Var	Var	112	113	119	120	126	127	132	133, 135	--	139	--
Off	30	Var	0	0	--	94	--	--	--	97	--	--	--	98	--
		0	Var	90	--	95	--	--	--	96	--	--	--	99	--
		+5	Var	Var	--	92	--	--	--	--	--	--	--	--	--
		-15	Var	Var	--	93	--	--	--	--	--	--	--	--	--

Note: Numbers in table under Mach number and total pressure represent part number.

NOMENCLATURE

CP	Pressure coefficient, $(P - P_\infty)/q_\infty$
M_∞	Free-stream Mach number
P	Local pressure, psfa
PT_∞	Free-stream total pressure, psfa
P_∞	Free-stream static pressure, psfa
q_∞	Free-stream dynamic pressure, psf
a_m	Model angle of attack, deg
a_s	Sensor angle of attack, deg
β_m	Model angle of sideslip, deg
β_s	Sensor angle of sideslip, deg
Λ_w	Wing sweep angle, deg
ϕ_m	Model roll angle, deg